LOW-TEMPERATURE TRANSPORT THROUGH A QUANTUM DOT

Leonid I. Glazman[1] and Michael Pustilnik[2]

[1] *William I. Fine Theoretical Physics Institute, University of Minnesota, Minneapolis, MN 55455, USA*
[2] *School of Physics, Georgia Institute of Technology, Atlanta, GA 30332, USA*

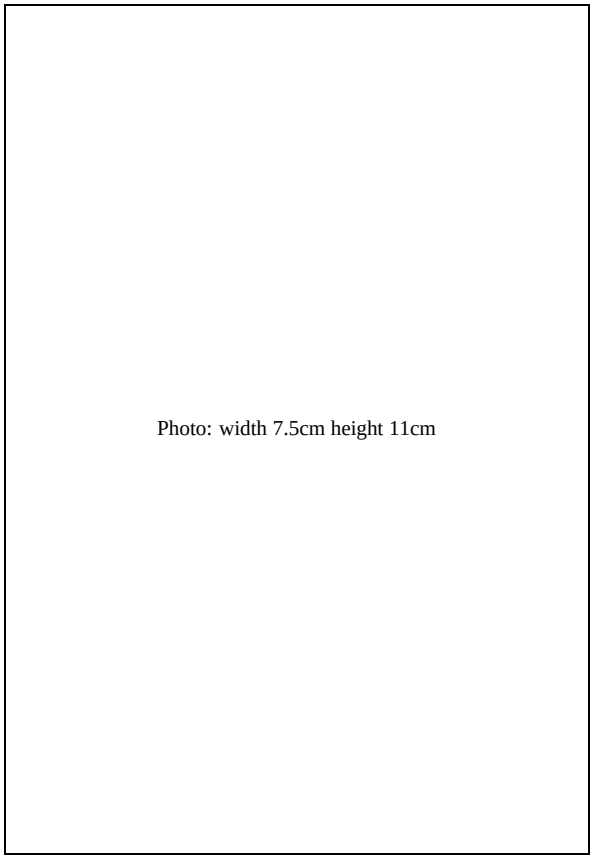
Photo: width 7.5cm height 11cm

Contents

Abstract

We review mechanisms of low-temperature electronic transport through a quantum dot weakly coupled to two conducting leads. Transport in this case is dominated by electron-electron interaction. At temperatures moderately lower than the charging energy of the dot, the linear conductance is suppressed by the Coulomb blockade. Upon further lowering of the temperature, however, the conductance may start to increase again due to the Kondo effect. We concentrate on lateral quantum dot systems and discuss the conductance in a broad temperature range, which includes the Kondo regime.

1. Introduction

In quantum dot devices [1] a small droplet of electron liquid, or just a few electrons are confined to a finite region of space. The dot can be attached by tunneling junctions to massive electrodes to allow electronic transport across the system. The conductance of such a device is determined by the number of electrons on the dot N, which in turn is controlled by varying the potential on the gate - an auxiliary electrode capacitively coupled to the dot [1]. At sufficiently low temperatures, N is an integer at almost any gate voltage V_g. Exceptions are narrow intervals of V_g in which an addition of a single electron to the dot does not change much the electrostatic energy of the system. Such a degeneracy between different charge states of the dot allows for an activationless electron transfer through it, whereas for all other values of V_g the activation energy for the conductance G across the dot is finite. The resulting oscillatory dependence $G(V_g)$ is the hallmark of the Coulomb blockade phenomenon [1]. The contrast between the low- and high-conductance regions (Coulomb blockade valleys and peaks, respectively) gets sharper at lower temperatures. The pattern of periodic oscillations in the G vs. V_g dependence is observed down to the lowest attainable temperatures in experiments on tunneling through small metallic islands [2].

Conductance through quantum dots formed in semiconductor heterostructures exhibits a reacher behavior [1]. In larger dots (in the case of GaAs heterostructures, such dots may contain hundreds of electrons), the fluctuations of the heights of the Coulomb blockade peaks become apparent already at moderately low temperatures. Characteristic for mesoscopic phenomena, the heights are sensitive to the shape of a dot and to the magnetic flux threading it. The separation in gate voltage between the Coulomb blockade peaks, and the conductance in the valleys also exhibit mesoscopic fluctuations. However, the pattern of sharp conductance peaks separating the low-conductance valleys of the $G(V_g)$ dependence persists. Smaller quantum dots (containing few tens of electrons in the case of GaAs) show yet another feature [4]: in some Coulomb blockade valleys the dependence $G(T)$ is not monotonic and has a minimum at a finite temperature. This minimum is similar in origin [5] to the well-known non-monotonic temperature dependence of the resistivity of a metal containing magnetic impurities [6] – the *Kondo effect*. Typically, the valleys with anomalous temperature dependence correspond to an odd number of electrons in the dot. In an ideal case, the low-temperature conductance in such a valley is of the order of conductance at peaks surrounding it. Thus, at low temperatures the two adjacent peaks merge to form a broad maximum.

The number of electrons on the dot is a well-defined quantity as long the conductances of the junctions connecting the dot to the electrodes is small compared to the conductance quantum e^2/h. In quantum dot devices formed in semi-

conductor heterostructures the conductances of junctions can be tuned continuously. With the increase of the conductances, the periodic pattern in $G(V_g)$ dependence gradually gives way to mesoscopic conductance fluctuations. Yet, electron-electron interaction still affects the transport through the device. A strongly asymmetric quantum dot device with one junction weakly conducting, while another completely open, provides a good example of that [7, 8, 9]. The differential conductance across the device in this case exhibits zero-bias anomaly – suppression at low bias. Clearly, Coulomb blockade is not an isolated phenomenon, but is closely related to interaction-induced anomalies of electronic transport and thermodynamics in higher dimensions [3].

The emphasis of these lectures is on the Kondo effect in quantum dots. We will concentrate on the so-called *lateral quantum dot systems* [1, 4], formed by gate depletion of a two-dimensional electron gas at the interface between two semiconductors. These devices offer the highest degree of tunability, yet allow for relatively simple theoretical treatment. At the same time, many of the results presented below are directly applicable to other systems as well, including vertical quantum dots [10, 11, 12], Coulomb-blockaded carbon nanotubes [12, 13], single-molecule transistors [14], and magnetic atoms on metallic surfaces [15].

Kondo effect emerges at relatively low temperature, and we will follow the evolution of the conductance upon the reduction of temperature. On the way to Kondo effect, we encounter also the phenomena of Coulomb blockade and of mesoscopic conductance fluctuations.

2. Model of a lateral quantum dot system

The Hamiltonian of interacting electrons confined to a quantum dot has the following general form,

$$H_{\rm dot} = \sum_s \sum_{ij} h_{ij} d^\dagger_{is} d_{js} + \frac{1}{2} \sum_{ss'} \sum_{ijkl} h_{ijkl} d^\dagger_{is} d^\dagger_{js'} d_{ks'} d_{ls}. \qquad (2.1)$$

Here an operator $d^\dagger_{is}$ creates an electron with spin s in the orbital state $\phi_i(\boldsymbol{r})$ (the wave functions are normalized according to $\int d\boldsymbol{r} \phi^*_i(\boldsymbol{r})\phi_j(\boldsymbol{r}) = \delta_{ij}$); $h_{ij} = h^*_{ji}$ is an Hermitian matrix describing the single-particle part of the Hamiltonian. The matrix elements h_{ijkl} depend on the potential $U(\boldsymbol{r}-\boldsymbol{r}')$ of electron-electron interaction,

$$h_{ijkl} = \int d\boldsymbol{r}\, d\boldsymbol{r}' \phi^*_i(\boldsymbol{r})\phi^*_j(\boldsymbol{r}')U(\boldsymbol{r}-\boldsymbol{r}')\phi_k(\boldsymbol{r}')\phi_l(\boldsymbol{r}). \qquad (2.2)$$

The Hamiltonian (2.1) can be simplified further provided that the quasiparticle spectrum is not degenerate near the Fermi level, that the Fermi-liquid theory

is applicable to the description of the dot, and that the dot is in the metallic conduction regime. The first of these conditions is satisfied if the dot has no spatial symmetries, which implies also that motion of quasiparticles within the dot is chaotic.

The second condition is met if the electron-electron interaction within the dot is not too strong, i.e. the gas parameter r_s is small,

$$r_s = (k_F a_0)^{-1} \lesssim 1, \quad a_0 = \kappa\hbar^2/e^2 m^* \tag{2.3}$$

Here k_F is the Fermi wave vector, a_0 is the effective Bohr radius, κ is the dielectric constant of the material, and m^* is the quasiparticle effective mass.

The third condition requires the ratio of the Thouless energy E_T to the mean single-particle level spacing δE to be large [16],

$$g = E_T/\delta E \gg 1. \tag{2.4}$$

For a ballistic two-dimensional dot of linear size L the Thouless energy E_T is of the order of $\hbar v_F/L$, whereas the level spacing can be estimated as

$$\delta E \sim \hbar v_F k_F/N \sim \hbar^2/m^* L^2. \tag{2.5}$$

Here v_F is the Fermi velocity and $N \sim (k_F L)^2$ is the number of electrons in the dot. Therefore,

$$g \sim k_F L \sim \sqrt{N}\,, \tag{2.6}$$

so that having a large number of electrons $N \gg 1$ in the dot guarantees that the condition Eq. (2.4) is satisfied.

Under the conditions (2.3), (2.4) the *Random Matrix Theory* (for a review see, e.g., [17, 18, 19, 20]) is a good starting point for description of non-interacting quasiparticles within the energy strip of the width E_T about the Fermi level [16]. The matrix elements h_{ij} in Eq. (2.1) belong to a Gaussian ensemble [19, 20]. Since the matrix elements do not depend on spin, each eigenvalue ϵ_n of the matrix h_{ij} represents a spin-degenerate energy level. The spacings $\epsilon_{n+1} - \epsilon_n$ between consecutive levels obey the Wigner-Dyson statistics [19]; the mean level spacing $\langle \epsilon_{n+1} - \epsilon_n \rangle = \delta E$.

We discuss now the second term in the Hamiltonian (2.1), which describes electron-electron interaction. It turns out [21, 22, 23] that the vast majority of the matrix elements h_{ijkl} are small. Indeed, in the lowest order in $1/g \ll 1$, the wave functions $\phi_i(\boldsymbol{r})$ are Gaussian random variables with zero mean, statistically independent of each other and of the corresponding energy levels [24]:

$$\overline{\phi_i^*(\boldsymbol{r})\phi_j(\boldsymbol{r}')} = \frac{\delta_{ij}}{\mathcal{A}}\, F(|\boldsymbol{r}-\boldsymbol{r}'|)\,, \quad \overline{\phi_i(\boldsymbol{r})\phi_j(\boldsymbol{r}')} = \frac{\delta_{\beta,1}\delta_{ij}}{\mathcal{A}}\, F(|\boldsymbol{r}-\boldsymbol{r}'|)\,. \tag{2.7}$$

Here $\mathcal{A} \sim L^2$ is the area of the dot, and the function F is given by

$$F(r) \sim \langle \exp(i\boldsymbol{k}\cdot\boldsymbol{r})\rangle_{\rm FS}\,. \tag{2.8}$$

where $\langle\ldots\rangle_{\rm FS}$ stands for the averaging over the Fermi surface $|\boldsymbol{k}| = k_F$. In two dimensions, the function $F(r)$ decreases with r as $F \propto (k_F r)^{-1/2}$ at $k_F r \gg 1$, and saturates to $F \sim 1$ at $k_F r \ll 1$.

The parameter β in Eq. (2.7) distinguishes between the presence $(\beta = 1)$ or absence $(\beta = 2)$ of the time-reversal symmetry. The symmetry breaking is driven by the orbital effect of the magnetic field and is characterised by the parameter

$$\chi = (\Phi/\Phi_0)\sqrt{g},$$

where Φ is the magnetic flux threading the dot and $\Phi_0 = hc/e$ is the flux quantum, so that the limits $\chi \ll 1$ and $\chi \gg 1$ correspond to, respectively, $\beta = 1$ and $\beta = 2$. Note that in the case of a magnetic field $H_\perp$ applied perpendicular to the plane of the dot, the crossover (at $\chi \sim 1$) between the two regimes occurs at so weak field that the corresponding Zeeman energy B is negligible[1].

After averaging with the help of Eqs. (2.7)-(2.8), the matrix elements (2.2) take the form

$$\overline{h_{ijkl}} = \big(2E_C + E_S/2\big)\delta_{il}\delta_{jk} + E_S\delta_{ik}\delta_{jl} + \Lambda\big(2/\beta - 1\big)\delta_{ij}\delta_{kl}.$$

We substitute this expression into Hamiltonian (2.1), and rearrange the sum over the spin indexes with the help of the identity

$$2\,\delta_{s_1 s_2}\delta_{s_1' s_2'} = \delta_{s_1 s_1'}\delta_{s_2' s_2} + \boldsymbol{\sigma}_{s_1 s_1'}\cdot\boldsymbol{\sigma}_{s_2' s_2}, \tag{2.9}$$

where $\boldsymbol{\sigma} = (\sigma^x, \sigma^y, \sigma^z)$ are the Pauli matrices. This results in a remarkably simple form [22, 23]

$$H_{\rm int} = E_C\hat{N}^2 - E_S\hat{\mathbf{S}}^2 + \Lambda\big(2/\beta - 1\big)\hat{T}^\dagger\hat{T} \tag{2.10}$$

of the interaction part of the Hamiltonian of the dot. Here

$$\hat{N} = \sum_{ns} d_{ns}^\dagger d_{ns}, \quad \hat{\mathbf{S}} = \sum_{nss'} d_{ns}^\dagger \frac{\boldsymbol{\sigma}_{ss'}}{2}\, d_{ns'} \quad \hat{T} = \sum_n d_{n\uparrow}^\dagger d_{n\downarrow}^\dagger \tag{2.11}$$

are the operators of the total number of electrons in the dot, of the dot's spin, and the "pair creation" operator corresponding to the interaction in the Cooper channel.

[1] For example, in the experiments [25] the crossover takes place at $H_\perp \sim 10\,mT$. Zeeman energy in such a field $B \sim 2.5\,mK$, which is by an order of magnitude lower than the base temperature in the measurements.

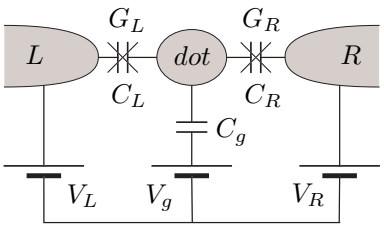

Fig. 1. Equivalent circuit for a quantum dot connected to two leads by tunnel junctions and capacitively coupled to the gate electrode. The total capacitance of the dot $C = C_L + C_R + C_g$.

The first term in Eq. (2.10) represents the electrostatic energy. In the conventional equivalent circuit picture, see Fig. 1, the charging energy E_C is related to the total capacitance C of the dot, $E_C = e^2/2C$. For a mesoscopic ($k_F L \gg 1$) conductor, the charging energy is large compared to the mean level spacing δE. Indeed, using the estimates $C \sim \kappa L$ and Eqs. (2.3) and (2.5), we find

$$E_C/\delta E \sim L/a_0 \sim r_s\sqrt{N}. \tag{2.12}$$

Except an exotic case of an extremely weak interaction, this ratio is large for $N \gg 1$; for the smallest quantum dots formed in GaAs heterostructures, $E_C/\delta E \sim 10$ [4]. Note that Eqs. (2.4), (2.6), and (2.12) imply that

$$E_T/E_C \sim 1/r_s \gtrsim 1,$$

which justifies the use of RMT for the description of single-particle states with energies $|\epsilon_n| \lesssim E_C$, relevant for Coulomb blockade.

The second term in Eq. (2.10) describes the intra-dot exchange interaction, with the exchange energy E_S given by

$$E_S = \int d\boldsymbol{r}\, d\boldsymbol{r}' U(\boldsymbol{r}-\boldsymbol{r}')F^2(|\boldsymbol{r}-\boldsymbol{r}'|) \tag{2.13}$$

In the case of a long-range interaction the potential U here should properly account for the screening [23]. For $r_s \ll 1$ the exchange energy can be estimated with logarithmic accuracy by substituting $U(r) = (e^2/\kappa r)\theta(a_0 - r)$ into Eq. (2.13) (here we took into account that the screening length in two dimensions coincides with the Bohr radius a_0), which yields

$$E_S \sim r_s \ln(1/r_S)\, \delta E \ll \delta E. \tag{2.14}$$

The estimate Eq. (2.14) is valid only for $r_s \ll 1$. However, the ratio $E_S/\delta E$

remains small for experimentally relevant[2] value $r_s \sim 1$ as long as the Stoner criterion for the absence of itinerant magnetism [26] is satisfied. This guarantees the absence of a macroscopic (proportional to N) magnetization of a dot in the ground state [22].

The third term in Eq. (2.10), representing interaction in the Cooper channel, is renormalized by higher-order corrections arising due to virtual transitions to states outside the energy strip of the width E_T about the Fermi level. For attractive interaction ($\Lambda < 0$) the renormalization enhances the interaction, eventually leading to the superconducting instability and formation of a gap Δ_Λ in the electronic spectrum. Properties of very small ($\Delta_\Lambda \sim \delta E$) superconducting grains are reviewed in, e.g., [27]; for properties of larger grains ($\Delta_\Lambda \sim E_C$) see [28]. Here we concentrate on the repulsive interaction ($\Lambda > 0$), in which case Λ is very small,

$$\Lambda \sim \frac{\delta E}{\ln(\epsilon_F/E_T)} \sim \frac{\delta E}{\ln N} \ll \delta E.$$

This estimate accounts for the logarithmic renormalization of Λ when the high-energy cutoff is reduced from the Fermi energy ϵ_F down to the Thouless energy E_T [23]. In addition, if the time-reversal symmetry is lifted ($\beta = 2$) then the third term in Eq. (2.10) is zero to start with. Accordingly, hereinafter we neglect this term altogether by setting $\Lambda = 0$.

Obviously, the interaction part of the Hamiltonian, Eq. (2.10), is invariant with respect to a change of the basis of single-particle states $\phi_i(\boldsymbol{r})$. Picking up the basis in which the first term in Eq. (2.1) is diagonal, we arrive at the *universal Hamiltonian* [22, 23],

$$H_{\rm dot} = \sum_{ns} \epsilon_n d_{ns}^\dagger d_{ns} + E_C\big(\hat{N} - N_0\big)^2 - E_S \hat{\mathbf{S}}^2. \qquad (2.15)$$

We included in Eq. (2.15) the effect of the capacitive coupling to the gate electrode: the dimensionless parameter N_0 is proportional to the gate voltage,

$$N_0 = C_g V_g / e,$$

where C_g is the capacitance between the dot and the gate, see Fig. 1. The relative magnitude of fully off-diagonal interaction terms in Eq. (2.1) (corresponding to h_{ijkl} with all four indices different), not included in Eq. (2.15), is of the order of $1/g \sim N^{-1/2} \ll 1$. Partially diagonal terms (two out of four indices coincide) are larger, of the order of $\sqrt{1/g} \sim N^{-1/4}$, but still are assumed to be negligible as $N \gg 1$.

[2] For GaAs ($m^* \approx 0.07 m_e$, $\kappa \approx 13$) the effective Bohr radius $a_0 \approx 10\ nm$, whereas a typical density of the two-dimensional electron gas, $n \sim 10^{11}\ cm^{-2}$ [4], corresponds to $k_F = \sqrt{2\pi n} \sim 10^6\ cm^{-1}$. This gives $k_F a_0 \sim 1$.

As discussed above, in this limit the energy scales involved in Eq. (2.15) form a well-defined hierarchy

$$E_S \ll \delta E \ll E_C. \tag{2.16}$$

If all the single-particle energy levels ϵ_n were equidistant, then the spin S of an even-N state would be zero, while an odd-N state would have $S = 1/2$. However, the level spacings are random. If the spacing between the highest occupied level and the lowest unoccupied one is accidentally small, than the gain in the exchange energy, associated with the formation of a higher-spin state, may be sufficient to overcome the loss of the kinetic energy (cf. the Hund's rule in quantum mechanics). For $E_S \ll \delta E$ such deviations from the simple even-odd periodicity are rare [22, 29, 30]. This is why the last term in Eq. (2.15) is often neglected. Eq. (2.15) then reduces to the Hamiltonian of the *Constant Interaction Model*, widely used in the analysis of experimental data [1]. Finally, it should be emphasized that SU(2)–invariant Hamiltonian (2.15) describes a dot in the absence of the spin-orbit interaction, which would destroy this symmetry.

Electron transport through the dot occurs via two dot-lead junctions. In a typical geometry, the confining potential forming a lateral quantum dot varies smoothly on the scale of the Fermi wavelength. Hence, the point contacts connecting the quantum dot to the leads act essentially as electronic waveguides. Potentials on the gates control the waveguide width, and, therefore, the number of electronic modes the waveguide support: by making the waveguide narrower one pinches the propagating modes off one-by-one. Each such mode contributes $2e^2/h$ to the conductance of a contact. The Coulomb blockade develops when the conductances of the contacts are small compared to $2e^2/h$, i.e. when the very last propagating mode approaches its pinch-off [31, 32]. Accordingly, in the Coulomb blockade regime each dot-lead junction in a lateral quantum dot system supports only a single electronic mode [33].

As discussed below, for $E_C \gg \delta E$ the characteristic energy scale relevant to the Kondo effect, the Kondo temperature T_K, is small compared to the mean level spacing: $T_K \ll \delta E$. This separation of the energy scales allows us to simplify the problem even further by assuming that the conductances of the dot-lead junctions are small. This assumption will not affect the properties of the system in the Kondo regime. At the same time, it justifies the use of the tunneling Hamiltonian for description of the coupling between the dot and the leads. The microscopic Hamiltonian of the system can then be written as a sum of three distinct terms,

$$H = H_{\rm leads} + H_{\rm dot} + H_{\rm tunneling}, \tag{2.17}$$

which describe free electrons in the leads, isolated quantum dot, and tunneling between the dot and the leads, respectively. The second term in Eq. (2.17), the

Hamiltonian of the dot $H_{\rm dot}$, is given by Eq. (2.15). We treat the leads as reservoirs of free electrons with continuous spectra ξ_k, characterized by constant density of states ν, same for both leads. Moreover, since the typical energies $\omega \lesssim E_C$ of electrons participating in transport through a quantum dot in the Coulomb blockade regime are small compared to the Fermi energy of the electron gas in the leads, the spectra ξ_k can be linearized near the Fermi level, $\xi_k = v_F k$; here k is measured from k_F. With only one electronic mode per junction taken into account, the first and the third terms in Eq. (2.17) have the form

$$H_{\rm leads} = \sum_{\alpha k s} \xi_k c^\dagger_{\alpha k s} c_{\alpha k s}, \quad \xi_k = -\xi_{-k}, \tag{2.18}$$

$$H_{\rm tunneling} = \sum_{\alpha k n s} t_{\alpha n}\, c^\dagger_{\alpha k s} d_{n s} + {\rm H.c.} \tag{2.19}$$

Here $t_{\alpha n}$ are tunneling matrix elements (tunneling amplitudes) "connecting" the state n in the dot with the state k in the lead α ($\alpha = R, L$ for the right/left lead).

Tunneling leads to a broadening of discrete levels in the dot. The width $\Gamma_{\alpha n}$ that level n acquires due to escape of an electron to lead α is given by

$$\Gamma_{\alpha n} = \pi\nu \left| t^2_{\alpha n} \right| \tag{2.20}$$

Randomness of single-particle states in the dot translates into the randomness of the tunneling amplitudes. Indeed, the amplitudes depend on the values of the electron wave functions at the points $\boldsymbol{r}_\alpha$ of the contacts, $t_{\alpha n} \propto \phi_n(\boldsymbol{r}_\alpha)$. For $k_F \left| \boldsymbol{r}_L - \boldsymbol{r}_R \right| \sim k_F L \gg 1$ the tunneling amplitudes [and, therefore, the widths (2.20)] in the left and right junctions are statistically independent of each other. Moreover, the amplitudes to different energy levels are also uncorrelated, see Eq. (2.7):

$$\overline{t^*_{\alpha n} t_{\alpha' n'}} = \frac{\Gamma_\alpha}{\pi\nu}\, \delta_{\alpha\alpha'} \delta_{nn'}, \quad \overline{t_{\alpha n} t_{\alpha' n'}} = \frac{\Gamma_\alpha}{\pi\nu}\, \delta_{\beta,1} \delta_{\alpha\alpha'} \delta_{nn'}, \tag{2.21}$$

The average value $\Gamma_\alpha = \overline{\Gamma_{\alpha n}}$ of the width is related to the conductance of the corresponding dot-lead junction

$$G_\alpha = \frac{4e^2}{\hbar} \frac{\Gamma_\alpha}{\delta E}\,. \tag{2.22}$$

In the regime of strong Coulomb blockade ($G_\alpha \ll e^2/h$), the widths are small compared to the level spacing, $\Gamma_\alpha \ll \delta E$, so that discrete levels in the dot are well defined. Note that statistical fluctuations of the widths $\Gamma_{\alpha n}$ are large, and the corresponding distribution function is not Gaussian. Indeed, using Eqs. (2.20)

and (2.21) it is straightforward [19, 20] to show that

$$P(\gamma) = \overline{\delta\left(\gamma - \Gamma_{\alpha n}/\Gamma_\alpha\right)} = \begin{cases} \dfrac{e^{-\gamma/2}}{\sqrt{2\pi\gamma}}, & \beta = 1 \\ e^{-\gamma}, & \beta = 2 \end{cases} \tag{2.23}$$

This expression is known as Porter-Thomas distribution [34].

3. Thermally-activated conduction

At high temperatures, $T \gg E_C$, charging energy is negligible compared to the thermal energy of electrons. Therefore the conductance of the device in this regime G_∞ is not affected by charging and, independently of the gate voltage, is given by

$$\frac{1}{G_\infty} = \frac{1}{G_L} + \frac{1}{G_R}. \tag{3.1}$$

Dependence on N_0 develops at lower temperatures, $T \lesssim E_C$. It turns out that the conductance is suppressed for all gate voltages except narrow regions (*Coulomb blockade peaks*) around half-integer values of N_0. We will demonstrate this now using the method of rate equations [35, 36].

3.1. Onset of the Coulomb blockade oscillations

We start with the regime of relatively high temperatures,

$$\delta E \ll T \ll E_C, \tag{3.2}$$

and assume that the gate voltage is tuned sufficiently close to one of the points of charge degeneracy,

$$|N_0 - N_0^*| \lesssim T/E_C \tag{3.3}$$

(here N_0^* is a half-integer number).

Condition (3.2) enables us to treat the discrete single-particle levels within the dot as a continuum with the density of states $1/\delta E$. Condition Eq. (3.3), on the other hand, allows us to take into account only two charge states of the dot which are almost degenerate in the vicinity of the Coulomb blockade peak. For N_0 close to N_0^* these are the state $|0\rangle$ with $N = N_0^* - 1/2$ electrons on the dot, and the state $|1\rangle$ with $N = N_0^* + 1/2$ electrons. According to Eqs. (2.15) and (3.3), the difference of electrostatic energies of these states (the energy cost to add an electron to the dot) is

$$E_+(N_0) = E_{|1\rangle} - E_{|0\rangle} = 2E_C(N_0^* - N_0) \lesssim T. \tag{3.4}$$

In addition to the constraints (3.2) and (3.3), we assume here that the inelastic electron relaxation rate within the dot $1/\tau_\epsilon$ is large compared to the escape rates $\Gamma_\alpha/\hbar$. In other words, transitions between discrete levels in the dot occur before the electron escapes to the leads[3]. Under this assumption the tunnelings across the two junctions can be treated independently of each other (this is known as *sequential tunneling* approximation).

With the help of the Fermi golden rule the current I_α from the lead α into the dot can be written as

$$I_\alpha = e\,\frac{2\pi}{\hbar}\sum_{kns}\left|t_{\alpha n}^2\right|\delta(\xi_k + eV_\alpha - \epsilon_n - E_+) \times\Big\{\mathcal{P}_0 f(\xi_k)[1-f(\epsilon_n)] - \mathcal{P}_1 f(\epsilon_n)[1-f(\xi_k)]\Big\}\,. \tag{3.5}$$

Here $\mathcal{P}_i$ is the probability to find the dot in the charge states $|i\rangle$ $(i = 0, 1)$, $f(\omega) = [\exp(\omega/T)+1]^{-1}$ is the Fermi function, and V_α is the electric potential on the lead α, see Fig. 1. In writing Eq. (3.5) we assumed that the distribution functions $f(\xi_k)$ and $f(\epsilon_n)$ are not perturbed. This is well justified provided that the relaxation rate $1/\tau_\epsilon$ exceeds the rate $\sim G_\infty|V_L - V_R|/e$ at which electrons pass through the dot. Replacing the summations over n and k in Eq. (3.5) by integrations over the corresponding continua, and making use of Eqs. (2.20) and (2.22), we find

$$I_\alpha = \frac{G_\alpha}{e}\big[\mathcal{P}_0 F(E_+ - eV_\alpha) - \mathcal{P}_1 F(eV_\alpha - E_+)\big], \quad F(\omega) = \frac{\omega}{e^{\omega/T}-1}\,. \tag{3.6}$$

In the steady state, the currents across the two junctions satisfy

$$I = I_L = -I_R. \tag{3.7}$$

Equations (3.6) and (3.7), supplemented by the obvious normalization condition $\mathcal{P}_0 + \mathcal{P}_1 = 1$, allow one to find the probabilities $\mathcal{P}_i$ and the current across the dot I in response to the applied bias $V = V_L - V_R$. This yields for the linear conductance across the dot [35]

$$G = \lim_{V\to 0} dI/dV = G_\infty \frac{E_C(N_0 - N_0^*)/T}{\sinh[2E_C(N_0 - N_0^*)/T]}\,. \tag{3.8}$$

Here $N_0 = N_0^*$ corresponds to the Coulomb blockade peak. At each peak, the conductance equals half of its high-temperature value G_∞, see Eq. (3.1). On the contrary, in the *Coulomb blockade valleys* ($N_0 \neq N_0^*$), the conductance falls off

[3]Note that a finite inelastic relaxation rate requires inclusion of mechanisms beyond the model Eq. (2.15), e.g., electron-phonon collisions.

exponentially with the decrease of temperature, and all the valleys behave exactly the same way. Note that the sequential tunneling approximation disregards any interference phenomena for electrons passing the dot. Accordingly, the result Eq. (3.8) is insensitive to a weak magnetic field.

3.2. Coulomb blockade peaks at low temperature

At temperatures below the single-particle level spacing in the dot δE, the activation energy for electron transport equals the difference between the ground state energies of the Hamiltonian (2.15) corresponding to two subsequent (integer) eigenvalues of N. Obviously, this difference includes, in addition to the electrostatic contribution $E_+(N_0)$, see Eq. (3.4), also a finite (and random) level spacing. As a result, the distance in N_0 between adjacent Coulomb blockade peaks is no longer 1, but contains a small fluctuating contribution of the order of $\delta E/E_C$. Mesoscopic fluctuations of spacings between the peaks are still subject of a significant disagreement between theory and experiments. We will not consider these fluctuations here (see [18] for a recent review), and discuss only the heights of the peaks.

We concentrate on the temperature interval

$$\Gamma_\alpha \ll T \ll \delta E, \tag{3.9}$$

which extends to lower temperatures the regime considered in the previous section, see Eq. (3.2), and on the gate voltages tuned to the vicinity of the Coulomb blockade peak, see Eq. (3.3). Just as above, the latter condition allows us to neglect all charge states except the two with the lowest energy, $|0\rangle$ and $|1\rangle$. Due to the second inequality in Eq. (3.9), the thermal broadening of single-particle energy levels in the dot can be neglected, and the states $|0\rangle$ and $|1\rangle$ coincide with the ground states of the Hamiltonian (2.15) with, respectively, $N = N_0^* - 1/2$ and $N = N_0^* + 1/2$ electrons in the dot. To be definite, consider the case when

$$N_0^* = N + 1/2 \tag{3.10}$$

with N being an even integer; for simplicity, we also neglect the exchange term in Eq. (2.15). Then $|0\rangle$ (with even number of electrons N) is the state in which all single particle levels below the Fermi level ($n < 0$) are doubly occupied. This state is, obviously, non-degenerate. The state $|1\rangle$ differs from $|0\rangle$ by an addition of a single electron on the Fermi level $n = 0$. The extra electron may be in two possible spin states, hence $|1\rangle$ is doubly degenerate; we denote the two components of $|1\rangle$ by $|s\rangle$ with $s =\uparrow, \downarrow$. As discussed below, the degeneracy eventually gives rise to the Kondo effect. However, at $T \gg \Gamma_\alpha$ [see Eq. (3.9)] the quantum coherence associated with the onset of the Kondo effect is not important,

and the rate equations approach can still be used to study the transport across the dot [36].

Applying the Fermi golden rule, we write the contribution of electrons with spin s to the electric current $I_{\alpha s}$ from lead α to the dot as

$$I_{\alpha s} = e\,\frac{2\pi}{\hbar}\,\left|t_{\alpha 0}^2\right| \sum_k \delta\left(\xi_k + eV_\alpha - \epsilon_0 - E_+\right)\Big\{\mathcal{P}_0 f(\xi_k) - \mathcal{P}_s\left[1 - f(\xi_k)\right]\Big\}$$

We now neglect ϵ_0 as it is small compared to E_+ (thereby neglecting the mesoscopic fluctuations of the position of the Coulomb blockade peak) and replace the summation over k by an integration. This yields

$$I_{\alpha s} = \frac{2e}{\hbar}\,\Gamma_{\alpha 0}\Big\{\mathcal{P}_0 f\left(E_+ - eV_\alpha\right) - \mathcal{P}_s f\left(eV_\alpha - E_+\right)\Big\}. \tag{3.11}$$

In the steady state the currents $I_{\alpha s}$ satisfy

$$I_{Ls} = -I_{Rs} = I/2 \tag{3.12}$$

(here we took into account that both projections of spin contribute equally to the total electric current across the dot I). Solution of Eqs. (3.11) and (3.12) subject to the normalization condition $\mathcal{P}_0 + \mathcal{P}_\uparrow + \mathcal{P}_\downarrow = 1$ results in [23]

$$G = \frac{4e^2}{\hbar}\frac{\Gamma_{L0}\Gamma_{R0}}{\Gamma_{L0}+\Gamma_{R0}}\,\left[\frac{-df/d\omega}{1+f(\omega)}\right]_{\omega=E_+(N_0)}. \tag{3.13}$$

The case of odd N in Eq. (3.10) is also described by Eq. (3.13) after replacement $E_+(N_0) \to -E_+(N_0)$.

There are several differences between Eq. (3.13) and the corresponding expression Eq. (3.8) valid in the temperature range (3.2). First of all, the maximum of the conductance Eq. (3.13) occurs at the gate voltage slightly (by an amount of the order of T/E_C) off the degeneracy point $N_0 = N_0^*$, and, more importantly, the shape of the peak is not symmetric about the maximum. This asymmetry is due to correlations in transport of electrons with opposite spins through a single discrete level in the dot. In the maximum, the function (3.13) takes value

$$G_{\rm peak} \sim \frac{e^2}{h}\frac{\Gamma_{L0}\Gamma_{R0}}{\Gamma_{L0}+\Gamma_{R0}}\,\frac{1}{T}\,. \tag{3.14}$$

Note that Eqs. (3.13) and (3.14) depend on the widths $\Gamma_{\alpha 0}$ of the energy level $n = 0$ rather then on the averages Γ_α over many levels in the dot, as in Eq. (3.8). As already discussed in Sec. 2, the widths $\Gamma_{\alpha 0}$ are related to the values of the electron wave functions at the position of the dot-lead contacts, and, therefore, are

random. Accordingly, the heights $G_{\rm peak}$ of the Coulomb blockade peaks exhibit strong mesoscopic fluctuations. In view of Eq. (2.23), the distribution function of $G_{\rm peak}$, see Eq. (3.14), is expected to be broad and strongly non-Gaussian, as well as very sensitive to the magnetic flux threading the dot. This is indeed confirmed by calculations [37, 38] and agrees with experimental data [25, 39]. The expression for the distribution function is rather cumbersome and we will not reproduce it here, referring the reader to the original papers [37, 38] and reviews [18, 20, 23]) instead.

An order-of-magnitude estimate of the average height of the peak can be obtained by replacing $\Gamma_{\alpha 0}$ in Eq. (3.14) by Γ_α, see Eq. (2.22), which yields

$$\overline{G_{\rm peak}} \sim G_\infty \frac{\delta E}{T}\,. \tag{3.15}$$

This is by a factor $\delta E/T$ larger than the corresponding figure $G_{\rm peak} = G_\infty/2$ for the temperature range (3.2), and may even approach the unitary limit ($\sim e^2/h$) at the lower end of the temperature interval (3.9). Interestingly, breaking of time-reversal symmetry results in an increase of the average conductance [23]. This increase is analogous to negative magnetoresistance due to weak localization in bulk systems [40], with the same physics involved.

4. Activationless transport through a blockaded quantum dot

According to the rate equations theory [35], at low temperatures, $T \ll E_C$, conduction through the dot is exponentially suppressed in the Coulomb blockade valleys. This suppression occurs because the process of electron transport through the dot involves a *real transition* to the state in which the charge of the dot differs by e from the thermodynamically most probable value. The probability of such fluctuation is proportional to $\exp\left(-E_C|N_0 - N_0^*|/T\right)$, which explains the conductance suppression, see Eq. (3.7). Going beyond the lowest-order perturbation theory in conductances of the dot-leads junctions G_α allows one to consider processes in which states of the dot with a "wrong" charge participate in the tunneling process as *virtual states*. The existence of these higher-order contributions to the tunneling conductance was envisioned already in 1968 by Giaever and Zeller [41]. The first quantitative theory of this effect, however, was developed much later [42].

The leading contributions to the activationless transport, according to [42], are provided by the processes of *inelastic and elastic co-tunneling*. Unlike the sequential tunneling, in the co-tunneling mechanism, the events of electron tunneling from one of the leads into the dot, and tunneling from the dot to the other lead occur as a single quantum process.

4.1. Inelastic co-tunneling

In the inelastic co-tunneling mechanism, an electron tunnels from a lead into one of the vacant single-particle levels in the dot, while it is an electron occupying some other level that tunnels out of the dot, see Fig. 2(a). As a result, transfer of charge e between the leads is accompanied by a simultaneous creation of an electron-hole pair in the dot.

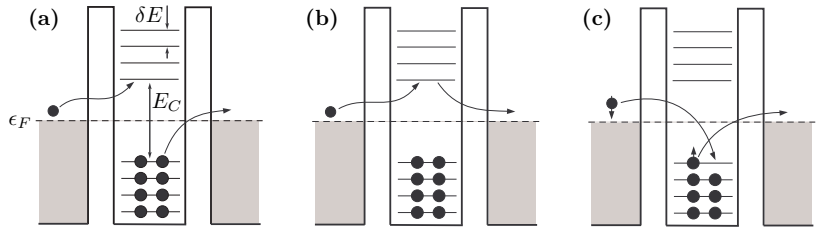

Fig. 2. Examples of the co-tunneling processes.
(a) inelastic co-tunneling: transferring of an electron between the leads leaves behind an electron-hole pair in the dot; (b) elastic co-tunneling; (c) elastic co-tunneling with a flip of spin.

Here we will estimate the contribution of the inelastic co-tunneling to the conductance deep in the Coulomb blockade valley, i.e. at almost integer N_0. Consider an electron that tunnels into the dot from the lead L. If energy ω of the electron relative to the Fermi level is small compared to the charging energy, $\omega \ll E_C$, then the energy of the virtual state involved in the co-tunneling process is close to E_C. The amplitude of the inelastic transition via this virtual state to the lead R is then given by

$$A_{n,m} = \frac{t^*_{Ln} t_{Rm}}{E_C}. \tag{4.1}$$

The initial state of this transition has an extra electron in the single-particle state k in the lead L, while the final state has an extra electron in the state k' in the lead R and an electron-hole pair in the dot (state n is occupied, state m is empty). The conductance is proportional to the sum of probabilities of all such processes,

$$G_{in} \sim \frac{e^2}{h} \sum_{n,m} \nu^2 \left| A^2_{n,m} \right| \sim \frac{e^2}{h} \frac{1}{E_C^2} \sum_{n,m} \Gamma_{Ln} \Gamma_{Rm}, \tag{4.2}$$

where we made use of Eq. (2.20). Now we estimate how many terms contribute to the sum in (4.2). Given the energy of the initial state ω, the number of available final states can be found from the phase space argument, familiar from the calculation of the quasiparticle lifetime in the Fermi liquid theory [43]. For $\omega \gg \delta E$

the energies of the states n and m lie within a strip of the width $\sim \omega/\delta E$ about the Fermi level. The total number of the final states contributing to the sum in Eq. (4.2) is then of the order of $(\omega/\delta E)^2$. Since the typical value of ω is T, the average value of the inelastic co-tunneling contribution to the conductance can be estimated as

$$\overline{G_{in}} \sim \left(\frac{T}{\delta E}\right)^2 \frac{e^2}{h}\frac{\Gamma_L\Gamma_R}{E_C^2}.$$

Using now Eq. (2.22), we find [42]

$$\overline{G_{in}} \sim \frac{G_L G_R}{e^2/h}\left(\frac{T}{E_C}\right)^2. \tag{4.3}$$

The terms entering the sum in Eq. (4.2) are random and uncorrelated. As it follows from Eq. (2.23), fluctuation of each term in the sum is of the order of its average value. This leads to the estimate for the fluctuation $\delta G_{in} = G_{in} - \overline{G_{in}}$ of the inelastic co-tunneling contribution to the conductance

$$\overline{\delta G_{in}^2} \sim \left(\frac{T}{\delta E}\right)^2 \left(\frac{e^2}{h}\frac{\Gamma_L\Gamma_R}{E_C^2}\right)^2 \sim \left(\frac{\delta E}{T}\right)^2 \left(\overline{G_{in}}\right)^2. \tag{4.4}$$

Accordingly, fluctuation of G_{in} is small compared to its average.

A comparison of Eq. (4.3) with the result of the rate equations theory (3.8) shows that the inelastic co-tunneling takes over the thermally-activated hopping at moderately low temperatures

$$T \lesssim T_{\rm in} = E_C\left[\ln\left(\frac{e^2/h}{G_L+G_R}\right)\right]^{-1}. \tag{4.5}$$

The smallest energy of an electron-hole pair is of the order of δE. At temperatures below this threshold the inelastic co-tunneling contribution is exponentially suppressed. It turns out, however, that even at much higher temperatures this mechanism becomes less effective than the elastic co-tunneling.

4.2. Elastic co-tunneling

In the process of elastic co-tunneling, transfer of charge between the leads is not accompanied by the creation of an electron-hole pair in the dot. In other words, occupation numbers of single-particle energy levels in the dot in the initial and final states of the co-tunneling process are exactly the same, see Fig. 2(b). Close to the middle of the Coulomb blockade valley (at almost integer N_0) the average number of electrons on the dot, $N \approx N_0$, is also an integer. Both an addition and a removal of a single electron cost E_C in electrostatic energy, see Eq. (2.15). The

amplitude of the elastic co-tunneling process in which an electron is transfered from lead L to lead R can then be written as

$$A_{el} = \sum_n t^*_{Ln} t_{Rn} \frac{\mathrm{sign}(\epsilon_n)}{E_C + |\epsilon_n|} \tag{4.6}$$

The two types of contributions to the amplitude A_{el} are associated with virtual creation of either an electron if the level n is empty ($\epsilon_n > 0$), or of a hole if the level is occupied ($\epsilon_n < 0$); the relative sign difference between the two types of contributions originates in the fermionic commutation relations.

As discussed in Sec. 2, the tunneling amplitudes $t_{\alpha n}$ entering Eq. (4.6) are Gaussian random variables with zero mean and variances given by Eq. (2.21). It is then easy to see that the second moment of the amplitude Eq. (4.6) is given by

$$\overline{|A^2_{el}|} = \frac{\Gamma_L \Gamma_R}{(\pi\nu)^2} \sum_n \big(E_C + |\epsilon_n|\big)^{-2}.$$

Since for $E_C \gg \delta E$ the number of terms making significant contribution to the sum over n here is large, and since the sum is converging, one can replace the summation by an integral which yields

$$\overline{|A^2_{el}|} \approx \frac{\Gamma_L \Gamma_R}{(\pi\nu)^2} \frac{1}{E_C \delta E}\,. \tag{4.7}$$

Substitution of this expression into

$$G_{el} = \frac{4\pi e^2 \nu^2}{\hbar} \left|A^2_{el}\right| \tag{4.8}$$

and making use of Eq. (2.22) gives [42]

$$\overline{G_{el}} \sim \frac{G_L G_R}{e^2/h} \frac{\delta E}{E_C}\,. \tag{4.9}$$

for the average value of the elastic co-tunneling contribution to the conductance.

This result is easily generalized to gate voltages tuned away from the middle of the Coulomb blockade valley. The corresponding expression reads

$$\overline{G_{el}} \sim \frac{G_L G_R}{e^2/h} \frac{\delta E}{E_C} \left(\frac{1}{N_0 - N_0^*} + \frac{1}{N_0^* - N_0 + 1} \right). \tag{4.10}$$

and is valid when N_0 is not too close to the degeneracy points $N_0 = N_0^*$ and $N_0 = N_0^* + 1$ (N_0^* is a half-integer number):

$$\min\big\{|N_0 - N_0^*|\,, |N_0 - N_0^* - 1|\big\} \gg \delta E / E_C$$

Comparison of Eq. (4.9) with Eq. (4.3) shows that the elastic co-tunneling mechanism dominates the electron transport already at temperatures

$$T \lesssim T_{el} = \sqrt{E_C \delta E}\,, \tag{4.11}$$

which may exceed significantly the level spacing. However, as we will see shortly below, mesoscopic fluctuations of G_{el} are strong [44], of the order of its average value. Thus, although $\overline{G_{el}}$ is always positive, see Eq. (4.10), the sample-specific value of G_{el} for a given gate voltage may vanish.

The key to understanding the statistical properties of the elastic co-tunneling contribution to the conductance is provided by the observation that there are many ($\sim E_C/\delta E \gg 1$) terms making significant contribution to the amplitude Eq. (4.6). All these terms are random and statistically independent of each other. The central limit theorem then suggests that the distribution of A_{el} is Gaussian [23], and, therefore, is completely characterised by the first two statistical moments,

$$\overline{A_{el}} = \overline{A^*_{el}}, \quad \overline{A_{el}A_{el}} = \overline{A^*_{el}A^*_{el}} = \delta_{\beta,1}\,\overline{A_{el}A^*_{el}} \tag{4.12}$$

with $\overline{A^*_{el}A_{el}}$ given by Eq. (4.7). This can be proven by explicit consideration of higher moments. For example,

$$\overline{|A^4_{el}|} = 2\Big(\overline{A_{el}A^*_{el}}\Big)^2 + \Big|\overline{A_{el}A_{el}}\Big|^2 + \delta\,\overline{|A^4_{el}|}. \tag{4.13}$$

The non-Gaussian correction here, $\delta\,\overline{|A^4_{el}|} \sim \overline{|A^2_{el}|}\,(\delta E/E_C)$, is by a factor of $\delta E/E_C \ll 1$ smaller than the main (Gaussian) contribution.

It follows from Eqs. (4.8), (4.12), and (4.13) that the fluctuation of the conductance $\delta G_{el} = G_{el} - \overline{G_{el}}$ satisfies

$$\overline{\delta G^2_{el}} = \frac{2}{\beta}\big(\overline{G_{el}}\,\big)^2\,. \tag{4.14}$$

Note that breaking of time reversal symmetry reduces the fluctuations by a factor of 2, similar to conductance fluctuations in bulk systems, whereas the average conductance (4.10) is not affected by the magnetic field.

It is clear from Eq. (4.14) that the fluctuations of the conductance are of the order of the conductance itself, despite naive expectations that the large number of the contributing states results in self-averaging. The reason is that one has to add amplitudes, rather than probabilities, in order to compute the conductance. Because the fluctuations of the conductance are large, its distribution function is not Gaussian. Given the statistics (4.12) of the amplitudes, it is not quite surprising that the distribution of G_{el} normalized to its average coincides

with Porter-Thomas distribution (2.23). This result was obtained first in [44] by a different (and more general) method.

Finally, it is interesting to compare the elastic co-tunneling contribution to the conductance fluctuations Eq. (4.14) with that of inelastic co-tunneling, see Eq. (4.4). Even though the inelastic co-tunneling is the main conduction mechanism at $T \gtrsim T_{el}$, see Eq. (4.11), elastic co-tunneling dominates the fluctuations of the conductance throughout the Coulomb blockade regime $T \lesssim E_C$.

5. Kondo regime in transport through a quantum dot

In the above discussion of the elastic co-tunneling we made a tacit assumption that all single-particle levels in the dot are either empty or doubly occupied. This, however, is not the case when the dot has a non-zero spin in the ground state. A dot with odd number of electrons, for example, would necessarily have a half-integer spin S. In the most important case of $S = 1/2$ the top-most occupied single-particle level is filled by a single electron and is spin-degenerate. This opens a possibility of a co-tunneling process in which a transfer of an electron between the leads is accompanied by a flip of electron's spin with simultaneous flip of the spin on the dot, see Fig. 2(c).

The amplitude of such a process, calculated in the fourth order in tunneling matrix elements, diverges logarithmically when the energy ω of an incoming electron approaches 0. Since $\omega \sim T$, the logarithmic singularity in the transmission amplitude translates into a dramatic enhancement of the conductance G across the dot at low temperatures: G may reach values as high as the quantum limit $2e^2/h$ [45, 46]. This conductance enhancement is not really a surprise. Indeed, in the spin-flip co-tunneling process a quantum dot with odd N behaves as $S = 1/2$ magnetic impurity embedded into a tunneling barrier separating two massive conductors [47]. It is known [48] since mid-60's that the presence of such impurities leads to zero-bias anomalies in tunneling conductance [49], which are adequately explained [50, 51] in the context of the Kondo effect [6].

5.1. Effective low-energy Hamiltonian

At energies well below the threshold $\Delta \sim \delta E$ for intra-dot excitations the transitions within the $(2S + 1)$-fold degenerate ground state manifold of a dot can be conveniently described by a spin operator $\mathbf{S}$. The form of the *effective Hamiltonian* describing the interaction of the dot with conduction electrons in the leads

is then dictated by SU(2) symmetry[4],

$$H_{\rm eff} = \sum_{\alpha k s} \xi_k c^\dagger_{\alpha k s} c_{\alpha k s} + \sum_{\alpha\alpha'} J_{\alpha\alpha'} (\mathbf{s}_{\alpha'\alpha} \cdot \mathbf{S}) \tag{5.1}$$

with $\mathbf{s}_{\alpha\alpha'} = \sum_{kk'ss'} c^\dagger_{\alpha k s} (\boldsymbol{\sigma}_{ss'}/2)\, c_{\alpha' k' s'}$. The sum over k in Eq. (5.1) is restricted to $|\xi_k| < \Delta$. The exchange amplitudes $J_{\alpha\alpha'}$ form 2×2 Hermitian matrix $\hat{J}$. The matrix has two real eigenvalues, the exchange constants J_1 and J_2 (hereafter we assume that $J_1 \geq J_2$). By an appropriate rotation in the $R-L$ space the Hamiltonian (5.2) can then be brought into the form

$$H_{\rm eff} = \sum_{\gamma k s} \xi_k \psi^\dagger_{\gamma k s} \psi_{\gamma k s} + \sum_{\gamma} J_\gamma (\mathbf{s}_\gamma \cdot \mathbf{S}). \tag{5.2}$$

Here the operators ψ_γ are certain linear combinations of the original operators $c_{R,L}$ describing electrons in the leads, and

$$\mathbf{s}_\gamma = \sum_{kk'ss'} \psi^\dagger_{\gamma k s} \frac{\boldsymbol{\sigma}_{ss'}}{2} \psi_{\gamma k' s'}$$

is local spin density of itinerant electrons in the "channel" $\gamma = 1, 2$.

The symmetry alone is not sufficient to determine the exchange constants J_γ; their evaluation must rely upon a microscopic model. Here we briefly outline the derivation [33, 52, 53] of Eq. (5.1) for a generic model of a quantum dot system discussed in Section 2 above. For simplicity, we will assume that the gate voltage N_0 is tuned to the middle of the Coulomb blockade valley. The tunneling (2.19) mixes the state with $N = N_0$ electrons on the dot with states having $N \pm 1$ electrons. The electrostatic energies of these states are high ($\sim E_C$), hence the transitions $N \to N \pm 1$ are virtual, and can be taken into account perturbatively in the second order in tunneling amplitudes [54].

For the Hamiltonian (2.15) the occupations of single-particle energy levels are good quantum numbers. Therefore, the amplitude $J_{\alpha\alpha'}$ can be written as a sum of partial amplitudes,

$$J_{\alpha\alpha'} = \sum_n J^n_{\alpha\alpha'}. \tag{5.3}$$

Each term in the sum here corresponds to a process during which an electron or a hole is created virtually on the level n in the dot, cf. Eq. (4.6). For $G_\alpha \ll e^2/h$ and $E_S \ll \delta E$ the main contribution to the sum in Eq. (5.3) comes from singly-occupied energy levels in the dot. A dot with spin S has $2S$ such levels near the

[4] In writing Eq. (5.1) we omitted the potential scattering terms associated with the usual elastic co-tunneling. This approximation is well justified when the conductances of the dot-lead junctions are small, $G_\alpha \ll e^2/h$, in which case G_{el} is also very small, see Eq. (4.7)

Fermi level (hereafter we assign indexes $n = -S, \ldots, n = S$ to these levels), each carrying a spin $\mathbf{S}/2S$, and contributing

$$J^n_{\alpha\alpha'} = \frac{\lambda_n}{E_C}\, t^*_{\alpha n} t_{\alpha' n}, \quad \lambda_n = 2/S, \quad |n| \le S \tag{5.4}$$

to the exchange amplitude in Eq. (5.1). This yields

$$J_{\alpha\alpha'} \approx \sum_{|n|\le S} J^n_{\alpha\alpha'}. \tag{5.5}$$

It follows from Equations (5.3) and (5.4) that

$$\mathrm{tr}\hat{J} = \frac{1}{E_C}\sum_n \lambda_n \left(|t^2_{Ln}| + |t^2_{Rn}|\right). \tag{5.6}$$

By restricting the sum over n here to $|n| \le S$, as in Eq. (5.5), and taking into account that all λ_n in Eq. (5.4) are positive, we find $J_1 + J_2 > 0$. Similarly, from

$$\det \hat{J} = \frac{1}{2E_C^2}\sum_{m,n} \lambda_m \lambda_n |\mathcal{D}^2_{mn}|, \quad \mathcal{D}_{mn} = \det \begin{pmatrix} t_{Lm} & t_{Rm} \\ t_{Ln} & t_{Rn} \end{pmatrix} \tag{5.7}$$

and Equations (5.4) and (5.5) follows that $J_1 J_2 > 0$ for $S > 1/2$. Indeed, in this case the sum in Eq. (5.7) contains at least one contribution with $m \ne n$; all such contributions are positive. Thus, both exchange constants $J_{1,2} > 0$ if the dot's spin S exceeds $1/2$ [33]. The peculiarities of the Kondo effect in quantum dots with large spin are discussed in Section 5.7 below.

We now turn to the most common case of $S = 1/2$ on the dot [4]. The ground state of such dot has only one singly-occupied energy level $(n = 0)$, so that $\det \hat{J} \approx 0$, see Eqs. (5.5) and (5.7). Accordingly, one of the exchange constants vanishes,

$$J_2 \approx 0, \tag{5.8}$$

while the remaining one, $J_1 = \mathrm{tr}\hat{J}$, is positive. Equation (5.8) resulted, of course, from the approximation made in Eq. (5.5). For the model (2.15) the leading correction to Eq. (5.5) originates in the co-tunneling processes with an intermediate state containing an extra electron (or an extra hole) on one of the empty (doubly-occupied) levels. Such contribution arises because the spin on the level n is not conserved by the Hamiltonian (2.15), unlike the corresponding occupation number. Straightforward calculation [52] yields the partial amplitude in the form of Eq. (5.4), but with

$$\lambda_n = -\frac{2E_C E_S}{(E_C + |\epsilon_n|)^2}, \qquad n \ne 0.$$

Unless the tunneling amplitudes $t_{\alpha 0}$ to the only singly-occupied level in the dot are anomalously small, the corresponding correction

$$\delta J_{\alpha\alpha'} = \sum_{n\neq 0} J^n_{\alpha\alpha'} \tag{5.9}$$

to the exchange amplitude (5.5) is small,

$$\left|\frac{\delta J_{\alpha\alpha'}}{J_{\alpha\alpha'}}\right| \sim \frac{E_S}{\delta E} \ll 1,$$

see Eq. (2.16). To obtain this estimate, we assumed that all tunneling amplitudes $t_{\alpha n}$ are of the same order of magnitude, and replaced the sum over n in Eq. (5.9) by an integral. A similar estimate yields the leading contribution to $\det \hat{J}$,

$$\det \hat{J} \approx \frac{1}{E_C^2}\sum_n \lambda_0\lambda_n|\mathcal{D}^2_{0n}| \sim -\frac{E_S}{\delta E}\big(\mathrm{tr}\hat{J}\big)^2,$$

or

$$J_2/J_1 \sim -E_S/\delta E. \tag{5.10}$$

According to Eq. (5.10), the exchange constant J_2 is negative [55], and its absolute value is small compared to J_1. Hence, Eq. (5.8) is indeed an excellent approximation for large chaotic dots with spin $S = 1/2$ as long as the intra-dot exchange interaction remains weak,[5] i.e. for $E_S \ll \delta E$. Note that corrections to the universal Hamiltonian (2.15) also result in finite values of both exchange constants, $|J_2| \sim J_1 N^{-1/2}$, and become important for small dots with $N \lesssim 10$ [46]. Although this may significantly affect the conductance across the system in the weak coupling regime $T \gtrsim T_K$, it does not lead to qualitative changes in the results for $S = 1/2$ on the dot, as the channel with smaller exchange constant decouples at low energies [56], see also Section 5.7 below. With this caveat, we adopt the approximation (5.8) in our description of the Kondo effect in quantum dots with spin $S = 1/2$. Accordingly, the effective Hamiltonian of the system (5.2) assumes the"block-diagonal" form

$$H_{\rm eff} = H_1 + H_2 \tag{5.11}$$

$$H_1 = \sum_{ks} \xi_k \psi^\dagger_{1ks}\psi_{1ks} + J(\mathbf{s}_1\cdot\mathbf{S}) \tag{5.12}$$

$$H_2 = \sum_{ks} \xi_k \psi^\dagger_{2ks}\psi_{2ks} \tag{5.13}$$

[5] Equation (5.8) holds identically for the Anderson impurity model [51] frequently employed to study transport through quantum dots. In that model a quantum dot is described by a single energy level, which formally corresponds to the infinite level spacing limit $\delta E \to \infty$ of the Hamiltonian (2.15).

with $J = \mathrm{tr}\hat{J} > 0$.

To get an idea about the physics of the Kondo model (see [57] for recent reviews), let us first replace the fermion field operator $\mathbf{s}_1$ in Eq. (5.12) by a single-particle spin-1/2 operator $\mathbf{S}_1$. The ground state of the resulting Hamiltonian of two spins

$$\widetilde{H} = J(\mathbf{S}_1 \cdot \mathbf{S})$$

is obviously a singlet. The excited state (a triplet) is separated from the ground state by the energy gap J_1. This separation can be interpreted as the binding energy of the singlet. Unlike $\mathbf{S}_1$ in this simple example, the operator $\mathbf{s}_1$ in Eq. (5.12) is merely a spin density of the conduction electrons at the site of the "magnetic impurity". Because conduction electrons are freely moving in space, it is hard for the impurity to "capture" an electron and form a singlet. Yet, even a weak local exchange interaction suffices to form a singlet ground state [58, 59]. However, the characteristic energy (an analogue of the binding energy) for this singlet is given not by the exchange constant J, but by the so-called Kondo temperature

$$T_K \sim \Delta \exp(-1/\nu J). \tag{5.14}$$

Using $\Delta \sim \delta E$ and Equations (5.6) and (2.22), one obtains from Eq. (5.14) the estimate

$$\ln\left(\frac{\delta E}{T_K}\right) \sim \frac{1}{\nu J} \sim \frac{e^2/h}{G_L + G_R}\frac{E_C}{\delta E}. \tag{5.15}$$

Since $G_\alpha \ll e^2/h$ and $E_C \gg \delta E$, the r.h.s. of Eq. (5.15) is a product of two large parameters. Therefore, the Kondo temperature T_K is small compared to the mean level spacing,

$$T_K \ll \delta E. \tag{5.16}$$

It is this separation of the energy scales that justifies the use of the effective low-energy Hamiltonian (5.1), (5.2) for the description of the Kondo effect in a quantum dot system. The inequality (5.16) remains valid even if the conductances of the dot-leads junctions G_α are of the order of $2e^2/h$. However, in this case the estimate (5.15) is no longer applicable [60].

In our model, see Equations (5.11)-(5.13), one of the channels (ψ_2) of conduction electrons completely decouples from the dot, while the ψ_1-particles are described by the standard single-channel antiferromagnetic Kondo model [6, 57]. Therefore, the thermodynamic properties of a quantum dot in the Kondo regime are identical to those of the conventional Kondo problem for a single magnetic impurity in a bulk metal; thermodynamics of the latter model is fully studied [61]. However, all the experiments addressing the Kondo effect in quantum dots test their transport properties rather then thermodynamics. The electron current operator is not diagonal in the (ψ_1, ψ_2) representation, and the contributions of these

two sub-systems to the conductance are not additive. Below we relate the linear conductance and, in some special case, the non-linear differential conductance as well, to the t-matrix of the conventional Kondo problem.

5.2. Linear response

The linear conductance can be calculated from the Kubo formula

$$G = \lim_{\omega\to 0} \frac{1}{\hbar\,\omega} \int_0^\infty dt\, e^{i\omega t} \Big\langle \big[\hat{I}(t), \hat{I}(0)\big] \Big\rangle, \tag{5.17}$$

where the current operator $\hat{I}$ is given by

$$\hat{I} = \frac{d}{dt}\frac{e}{2}\big(\hat{N}_R - \hat{N}_L\big), \quad \hat{N}_\alpha = \sum_{ks} c^\dagger_{\alpha ks} c_{\alpha ks} \tag{5.18}$$

Here $\hat{N}_\alpha$ is the operator of the total number of electrons in the lead α. Evaluation of the linear conductance proceeds similarly to the calculation of the impurity contribution to the resistivity of dilute magnetic alloys (see, e.g., [62]). In order to take the full advantage of the decomposition (5.11)-(5.13), we rewrite $\hat{I}$ in terms of the operators $\psi_{1,2}$. These operators are related to the original operators $c_{R,L}$ representing the electrons in the right and left leads via

$$\begin{pmatrix} \psi_{1ks} \\ \psi_{2ks} \end{pmatrix} = \begin{pmatrix} \cos\theta_0 & \sin\theta_0 \\ -\sin\theta_0 & \cos\theta_0 \end{pmatrix} \begin{pmatrix} c_{Rks} \\ c_{Lks} \end{pmatrix}. \tag{5.19}$$

The rotation matrix here is the same one that diagonalizes matrix $\hat{J}$ of the exchange amplitudes in Eq. (5.1); the rotation angle θ_0 satisfies the equation $\tan\theta_0 = |t_{L0}/t_{R0}|$. With the help of Eq. (5.19) we obtain

$$\hat{N}_R - \hat{N}_L = \cos(2\theta_0)\big(\hat{N}_1 - \hat{N}_2\big) - \sin(2\theta_0)\sum_{ks}\big(\psi^\dagger_{1ks}\psi_{2ks} + \text{H.c.}\big) \tag{5.20}$$

The current operator $\hat{I}$ entering the Kubo formula (5.17) is to be calculated with the equilibrium Hamiltonian (5.11)-(5.13). Since both $\hat{N}_1$ and $\hat{N}_2$ commute with $H_{\rm eff}$, the first term in Eq. (5.20) makes no contribution to $\hat{I}$. When the second term in Eq. (5.20) is substituted into Eq. (5.18) and then into the Kubo formula (5.17), the result, after integration by parts, can be expressed via 2-particle correlation functions such as $\big\langle \psi^\dagger_1(t)\psi_2(t)\psi^\dagger_2(0)\psi_1(0)\big\rangle$ (see Appendix B of [63] for further details about this calculation). Due to the block-diagonal structure of $H_{\rm eff}$, see Eq. (5.11), these correlation functions factorize into products of the

single-particle correlation functions describing the (free) ψ_2-particles and the (interacting) ψ_1-particles. The result of the evaluation of the Kubo formula can then be written as

$$G = G_0 \int d\omega \left(-\frac{df}{d\omega}\right) \frac{1}{2} \sum_s \left[-\pi\nu \,\mathrm{Im}\, T_s(\omega)\right]. \tag{5.21}$$

Here

$$G_0 = \frac{2e^2}{h} \sin^2(2\theta_0) = \frac{2e^2}{h} \frac{4|t_{L0}^2 t_{R0}^2|}{\left(|t_{L0}^2| + |t_{R0}^2|\right)^2}, \tag{5.22}$$

$f(\omega)$ is the Fermi function, and $T_s(\omega)$ is the t-matrix for the Kondo model (5.12). The t-matrix is related to the exact retarded Green function of the ψ_1-particles in the conventional way,

$$G_{ks,k's}(\omega) = G_k^0(\omega) + G_k^0(\omega) T_s(\omega) G_{k'}^0(\omega), \quad G_k^0 = (\omega - \xi_k + i0)^{-1}.$$

Here $G_{ks,k's}(\omega)$ is the Fourier transform of $G_{ks,k's}(t) = -i\theta(t)\left\langle \left\{ \psi_{1ks}(t), \psi_{1k's}^\dagger \right\} \right\rangle$, where $\langle \ldots \rangle$ stands for the thermodynamic averaging with the Hamiltonian (5.12). In writing Eq. (5.21) we took into account the conservation of the total spin (which implies that $G_{ks,k's'} = \delta_{ss'} G_{ks,k's}$, and that the interaction in Eq. (5.12) is local (which in turn means that the t-matrix is independent of k and k').

5.3. Weak coupling regime: $T_K \ll T \ll \delta E$

When the exchange term in the Hamiltonian (5.12) is treated perturbatively, the main contribution to the t-matrix comes from the transitions of the type [64]

$$|ks, \sigma\rangle \to |k's', \sigma'\rangle \,. \tag{5.23}$$

Here the state $|ks, \sigma\rangle$ has an extra electron with spin s in the orbital state k whereas the dot is in the spin state σ. By SU(2) symmetry, the amplitude of the transition (5.23) satisfies

$$A_{|k's',\sigma'\rangle \leftarrow |ks,\sigma\rangle} = A(\omega) \frac{1}{4} \left(\sigma_{\mathbf{s's}} \cdot \sigma_{\sigma'\sigma}\right) \tag{5.24}$$

Note that the amplitude is independent of k, k' because the interaction is local. However, it may depend on ω due to retardation effects.

The transition (5.23) is *elastic* in the sense that the number of quasiparticles in the final state of the transition is the same as that in the initial state (in other words, the transition (5.23) is not accompanied by the production of electron-hole pairs). Therefore, the imaginary part of the t-matrix can be calculated with

the help of the optical theorem [65], which yields

$$-\pi\nu\,\mathrm{Im}\,T_s = \frac{1}{2}\sum_{\sigma}\sum_{s'\sigma'}\left|\pi\nu\,A^2_{|k's',\sigma'\rangle\leftarrow|ks,\sigma\rangle}\right| . \tag{5.25}$$

The factor $1/2$ here accounts for the probability to have spin σ on the dot in the initial state of the transition. Substitution of the tunneling amplitude in the form (5.24) into Eq. (5.25), and summation over the spin indexes with the help of the identity (2.9) result in

$$-\pi\nu\,\mathrm{Im}\,T_s = \frac{3\pi^2}{16}\,\nu^2\big|A^2(\omega)\big| . \tag{5.26}$$

In the leading (first) order in J one readily obtains $A^{(1)} = J$, independently of ω. However, as discovered by Kondo [6], the second-order contribution $A^{(2)}$ not only depends on ω, but is logarithmically divergent as $\omega \to 0$:

$$A^{(2)}(\omega) = \nu J^2 \ln|\Delta/\omega| .$$

Here Δ is the high-energy cutoff in the Hamiltonian (5.12). It turns out [64] that similar logarithmically divergent contributions appear in all orders of perturbation theory,

$$\nu A^{(n)}(\omega) = (\nu J)^n \big[\ln|\Delta/\omega|\big]^{n-1},$$

resulting in a geometric series

$$\nu A(\omega) = \sum_{n=1}^{\infty}\nu A^{(n)} = \nu J\sum_{n=0}^{\infty}\big[\nu J\ln|\Delta/\omega|\big]^n = \frac{\nu J}{1-\nu J\ln|\Delta/\omega|} .$$

With the help of Eq. (5.14) this can be written as

$$\nu A(\omega) = \frac{1}{\ln|\omega/T_K|} . \tag{5.27}$$

Substitution of Eq. (5.27) into Eq. (5.26) and then into Eq. (5.21), and evaluation of the integral over ω with logarithmic accuracy yield for the conductance across the dot

$$G = G_0\frac{3\pi^2/16}{\ln^2(T/T_K)} , \quad T \gg T_K. \tag{5.28}$$

Equation (5.28) is the leading term of the asymptotic expansion in powers of $1/\ln(T/T_K)$, and represents the conductance in the *leading logarithmic approximation*.

Equation Eq. (5.28) resulted from summing up the most-diverging contributions in all orders of perturbation theory. It is instructive to re-derive it now in the framework of *renormalization group* [66]. The idea of this approach rests on the observation that the electronic states that give a significant contribution to observable quantities, such as conductance, are states within an interval of energies of the width $\omega \sim T$ about the Fermi level, see Eq. (5.21). At temperatures of the order of T_K, when the Kondo effect becomes important, this interval is narrow compared to the width of the band $D = \Delta$ in which the Hamiltonian (5.12) is defined.

Consider a narrow strip of energies of the width $\delta D \ll D$ near the edge of the band. Any transition (5.23) between a state near the Fermi level and one of the states in the strip is associated with high ($\sim D$) energy deficit, and, therefore, can only occur virtually. Obviously, virtual transitions via each of the states in the strip result in the second-order correction $\sim J^2/D$ to the amplitude $A(\omega)$ of the transition between states in the vicinity of the Fermi level. Since the strip contains $\nu\delta D$ electronic states, the total correction is [66]

$$\delta A \sim \nu J^2 \delta D/D.$$

This correction can be accounted for by modifying the exchange constant in the effective Hamiltonian $\widetilde{H}_{\rm eff}$ which is defined for states within a narrower energy band of the width $D - \delta D$ [66],

$$\widetilde{H}_{\rm eff} = \sum_{ks} \xi_k \psi^\dagger_{ks}\psi_{ks} + J_{D-\delta D}(\mathbf{s}_\psi \cdot \mathbf{S}), \quad |\xi_k| < D - \delta D, \tag{5.29}$$

$$J_{D-\delta D} = J_D + \nu J_D^2 \frac{\delta D}{D}. \tag{5.30}$$

Here J_D is the exchange constant in the original Hamiltonian. Note that the $\widetilde{H}_{\rm eff}$ has the same form as Eq. (5.12). This is not merely a conjecture, but can be shown rigorously [59, 67].

The reduction of the bandwidth can be considered to be a result of a unitary transformation that decouples the states near the band edges from the rest of the band [68]. In principle, any such transformation should also affect the operators that describe the observable quantities. Fortunately, this is not the case for the problem at hand. Indeed, the angle θ_0 in Eq. (5.19) is not modified by the transformation. Therefore, the current operator and the expression for the conductance (5.21) retain their form.

Successive reductions of the high-energy cutoff D by small steps δD can be viewed as a continuous process during which the initial Hamiltonian (5.12) with $D = \Delta$ is transformed to an effective Hamiltonian of the same form that acts within the band of the reduced width $D \ll \Delta$. It follows from Eq. (5.30) that the

dependence of the effective exchange constant on D is described by the differential equation [66, 67]

$$\frac{dJ_D}{d\zeta} = \nu J_D^2, \quad \zeta = \ln(\Delta/D)\,. \tag{5.31}$$

With the help of Eq. (5.14), the solution of the RG equation (5.31) subject to the initial condition $J_\Delta = J$ can be cast into the form

$$\nu J_D = \frac{1}{\ln(D/T_K)}\,. \tag{5.32}$$

The renormalization described by Eq. (5.31) can be continued until the bandwidth D becomes of the order of the typical energy $|\omega| \sim T$ for real transitions. After this limit has been reached, the transition amplitude $A(\omega)$ is calculated in lowest (first) order of perturbation theory in the effective exchange constant (higher order contributions are negligible for $D \sim \omega$),

$$\nu A(\omega) = \nu J_{D\sim|\omega|} = \frac{1}{\ln|\omega/T_K|}$$

Using now Eqs. (5.26) and (5.21), we recover Eq. (5.28).

5.4. Strong coupling regime: $T \ll T_K$

As temperature approaches T_K, the leading logarithmic approximation result Eq. (5.28) diverges. This divergence signals the failure of the approximation. Indeed, we are considering a model with single-mode junctions between the dot and the leads. The maximal possible conductance in this case is $2e^2/h$. To obtain a more precise bound, we discuss in this section the conductance in the strong coupling regime $T \ll T_K$.

We start with the zero-temperature limit $T = 0$. As discussed above, the ground state of the Kondo model (5.12) is a singlet [58], and, accordingly, is not degenerate. Therefore, the t-matrix of the conduction electrons interacting with the localized spin is completely characterized by the scattering phase shifts δ_s for electrons with spin s at the Fermi level. The t-matrix is then given by the standard scattering theory expression [65]

$$-\pi\nu\, T_s(0) = \frac{1}{2i}\,(\mathbb{S}_s - 1)\,, \quad \mathbb{S}_s = e^{2i\delta_s}\,, \tag{5.33}$$

where $\mathbb{S}_s$ is the scattering matrix for electrons with spin s, which for a single channel case reduces to its eigenvalue. Substitution of Eq. (5.33) into Eq. (5.21) yields

$$G(0) = G_0 \frac{1}{2}\sum_s \sin^2\delta_s \tag{5.34}$$

for the conductance, see Eq. (5.21). The phase shifts in Eqs. (5.33), (5.34) are obviously defined only $\mathrm{mod}\,\pi$ (that is, δ_s and $\delta_s + \pi$ are equivalent). This ambiguity can be removed if we set to zero the values of the phase shifts at $J = 0$ in Eq. (5.12).

In order to find the two phase shifts δ_s, we need two independent relations. The first one follows from the invariance of the Kondo Hamiltonian (5.12) under the particle-hole transformation $\psi_{ks} \to s\psi^\dagger_{-k,-s}$ (here $s = \pm 1$ for spin-up/down electrons). The particle-hole symmetry implies the relation for the t-matrix

$$T_s(\omega) = -T^*_{-s}(-\omega), \tag{5.35}$$

valid at all ω and T. In view of Eq. (5.33), it translates into the relation for the phase shifts at the Fermi level ($\omega = 0$) [69],

$$\delta_\uparrow + \delta_\downarrow = 0. \tag{5.36}$$

The second relation follows from the requirement that the ground state of the Hamiltonian (5.12) is a singlet [69]. In the absence of exchange ($J = 0$) and at $T = 0$, an infinitesimally weak (with Zeeman energy $B \to +0$) magnetic field

$$H_B = BS^z \tag{5.37}$$

would polarize the dot's spin. Since free electron gas has zero spin in the ground state, the total spin in a very large but finite region of space $\mathcal{V}$ surrounding the dot coincides with the spin of the dot, $\langle S^z\rangle_{J=0} = -1/2$. If the exchange with electron gas is now turned on, $J > 0$, a very weak field will not prevent the formation of a singlet ground state. In this state, the total spin within $\mathcal{V}$ is zero. Such change of the spin is possible if the numbers of spin-up and spin-down electrons within $\mathcal{V}$ have changed to compensate for the dot's spin: $\delta N_\uparrow - \delta N_\downarrow = 1$. By the Friedel sum rule, δN_s are related to the scattering phase shifts at the Fermi level, $\delta N_s = \delta_s/\pi$, which gives

$$\delta_\uparrow - \delta_\downarrow = \pi. \tag{5.38}$$

Combining Eqs. (5.36) and (5.38), we find

$$\delta_s = s\frac{\pi}{2}\,. \tag{5.39}$$

Equation (5.34) then yields for zero-temperature and zero-field conductance across the dot [45]

$$G(0) = G_0. \tag{5.40}$$

Thus, the grow of the conductance with lowering the temperature is limited only by the value of G_0. This value, see Eq. (5.22), depends only on the ratio of the

tunneling amplitudes $|t_{L0}/t_{R0}|$; if $|t_{L0}| = |t_{R0}|$, then the conductance at $T = 0$ will reach the maximal value $G = 2e^2/h$ allowed by quantum mechanics [45].

As explained above, screening of the dot's spin by itinerant electrons amounts to $\pm\pi/2$ phase shifts for electrons at the Fermi level ($\omega = 0$). However, the phase shifts at a finite ω deviate from the unitary limit value. Such deviation is to be expected, as the Kondo "resonance" has a finite width $\sim T_K$. There is also an inelastic component of scattering appearing at finite ω. Virtual transitions to excited states, corresponding to a broken up Kondo singlet, induce a local repulsive interaction between itinerant electrons [69], which is the cause of inelastic scattering. This interaction enters the fixed-point Hamiltonian, applicable when the relevant energies are small compared to the Kondo temperature T_K. The fixed point Hamiltonian takes a relatively simple form [69] when written in the basis of electronic states that incorporate an extra $\pm\pi/2$ phase shift [see Eq. (5.39)] compared to the original basis of Eq. (5.12). In the new basis,

$$H_{\text{fixed point}} = \sum_{ks} \xi_k \varphi^\dagger_{ks}\varphi_{ks} - \sum_{kk's} \frac{\xi_k + \xi_{k'}}{2\pi\nu T_K}\, \varphi^\dagger_{ks}\varphi_{k's} + \frac{1}{\pi\nu^2 T_K}\, \rho_\uparrow \rho_\downarrow . \quad (5.41)$$

Here $\rho_s = \sum_{kk'} {:}\varphi^\dagger_{ks}\varphi_{k's}{:}$ (the colons denote the normal ordering). The form of the last two terms in the r.h.s. of Eq. (5.41) is dictated by the particle-hole symmetry [69]. The ratio of their coefficients is fixed by the physical requirement that the Kondo singularity is tied to the Fermi level [69] (i.e. that the phase shifts depend only on the distance ω to the Fermi level), while the overall coefficient $1/T_K$ can be viewed as a precise definition of the Kondo temperature[6]. Note that by construction, the t-matrix for $\varphi-$particles $\widetilde{T}$ vanishes for $\omega = T = 0$.

The second term in the r.h.s. of Eq. (5.41) describes a purely elastic scattering, and yields a small $\omega-$dependent phase shift [69]

$$\widetilde{\delta}(\omega) = \frac{\omega}{T_K}\,. \quad (5.42)$$

The last term in Eq. (5.41) gives rise to an inelastic contribution to $\widetilde{T}$. Evaluation of this contribution in the second order of perturbation theory (see [62, 69] for details) results in

$$-\pi\nu\,\widetilde{T}_{in}(\omega) = i\,\frac{\omega^2 + \pi^2 T^2}{2\,T_K^2}\,. \quad (5.43)$$

In order to obtain the t-matrix in the original basis $T_s(\omega)$, we note that the elastic scattering phase shifts here are obtained by simply adding $\pm\pi/2$ to $\widetilde{\delta}$, i.e.

$$\delta_s(\omega) = s\frac{\pi}{2} + \widetilde{\delta}(\omega). \quad (5.44)$$

[6]With this convention the RG expression Eq. (5.14) is regarded as an estimate of T_K with logarithmic accuracy.

The relation between $T_s(\omega)$ and $\widetilde{T}(\omega)$, accounting for small inelastic term $\widetilde{T}_{in}$, reads

$$-\pi\nu T_s(\omega) = \frac{1}{2i}\left[e^{2i\delta_s(\omega)} - 1\right] + e^{2i\delta_s(\omega)}\left[-\pi\nu\,\widetilde{T}_{in}(\omega)\right]. \tag{5.45}$$

Note that the inelastic contribution enters this expression with an extra factor of $\exp(2i\delta_s)$. The appearance of this factor is a direct consequence of the unitarity of the scattering matrix in the presence of both elastic and inelastic scattering channels, see [69]. Taking into account Eqs. (5.42), (5.43), and (5.44), we find

$$-\pi\nu\,\mathrm{Im}\,T_s(\omega) = 1 - \frac{3\omega^2 + \pi^2 T^2}{2\,T_K^2}\,. \tag{5.46}$$

Substitution of this expression into Eq. (5.21) then yields

$$G = G_0\left[1 - (\pi T/T_K)^2\right], \quad T \ll T_K\,. \tag{5.47}$$

Accordingly, corrections to the conductance are quadratic in temperature – a typical Fermi liquid result [69]. The weak-coupling ($T \gg T_K$) and the strong-coupling ($T \ll T_K$) asymptotes of the conductance have a strikingly different structure. Nevertheless, since the Kondo effect is a crossover phenomenon rather than a phase transition [57, 58, 59, 61], the dependence $G(T)$ is a smooth and featureless [70] function throughout the crossover region $T \sim T_K$.

Finally, note that both Eqs. (5.28) and (5.47) have been obtained here for the particle-hole symmetric model (5.12). This approximation is equivalent to neglecting the elastic co-tunneling contribution to the conductance G_{el}. The asymptotes (5.28), (5.47) remain valid [33] as long as $G_{el}/G_0 \ll 1$. The overall temperature dependence of the linear conductance in the middle of the Coulomb blockade valley is sketched in Fig. 3.

The fixed point Hamiltonian (5.41) also allows one to calculate the corrections to zero-temperature conductance due to a finite magnetic field, which enters Eq. (5.41) via a term $H_B = \sum_{ks}(s/2)B\,\varphi^\dagger_{ks}\varphi_{ks}$. The field polarizes the electron gas, and the operators ρ_s acquire non-zero ground state expectation value $\langle\rho_s\rangle = -\nu Bs/2$. In order to calculate the phase shifts at the Fermi energy we replace $\rho_\uparrow\rho_\downarrow$ in the third term in the r.h.s. (5.41) by $\sum_s\langle\rho_{-s}\rangle\rho_s$, and $\xi_k, \xi_{k'}$ in the second term by their values at the Fermi level $\xi_k = -Bs/2$. As a result, Eq. (5.41) simplifies to

$$H = \sum_{ks}(\xi_k + \frac{s}{2}B)\varphi^\dagger_{ks}\varphi_{ks} + \sum_{kk's}\frac{Bs}{\pi\nu T_K}\,\rho_s,$$

from which one can read off the scattering phase shifts for $\varphi-$particles,

$$\widetilde{\delta}_s = -sB/T_K.$$

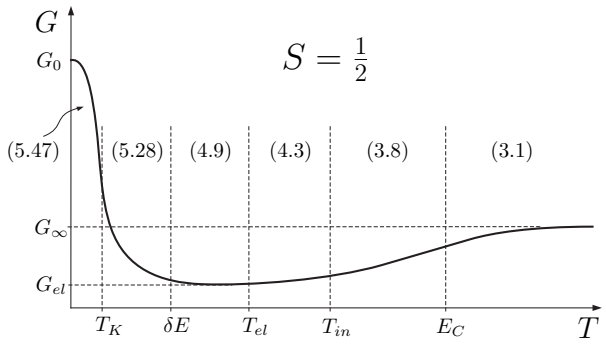

Fig. 3. Sketch of the temperature dependence of the conductance in the middle of the Coulomb blockade valley with $S = 1/2$ on the dot. The numbers in brackets refer to the corresponding equations in the text.

The phase shifts in the original basis are given by [69]

$$\delta_s = s\frac{\pi}{2} + \widetilde{\delta}_s = s\left(\frac{\pi}{2} - \frac{B}{T_K}\right),$$

cf. Eq. (5.44). Equation (5.34) then gives

$$G = G_0\left[1 - (B/T_K)^2\right], \quad B \ll T_K\,. \tag{5.48}$$

Note that the effect of a finite magnetic field on zero-temperature conductance is very similar to that a finite temperature has on the conductance at zero field, see Eq. (5.47). The similarity is not limited to the strong coupling regime. Indeed, the counterpart of Eq. (5.28) reads

$$G = G_0\frac{\pi^2/16}{\ln^2(B/T_K)}\,, \quad B \gg T_K. \tag{5.49}$$

5.5. Beyond linear response

In order to study transport through a quantum dot away from equilibrium we add to the effective Hamiltonian (5.11)-(5.13) a term

$$H_V = \frac{eV}{2}\left(\hat{N}_L - \hat{N}_R\right) \tag{5.50}$$

describing a finite voltage bias V applied between the left and right electrodes. Here we will evaluate the current across the dot at arbitrary V but under the

simplifying assumption that the dot-lead junctions are strongly asymmetric:

$$G_L \ll G_R.$$

Under this condition the angle θ_0 in Eq. (5.19) is small, $\theta_0 \approx |t_{L0}/t_{R0}| \ll 1$. Expanding Eq. (5.20) to linear order in θ_0 we obtain

$$H_V(\theta_0) = \frac{eV}{2}\big(\hat{N}_2 - \hat{N}_1\big) + eV\theta_0 \sum_{ks}\big(\psi^\dagger_{1ks}\psi_{2ks} + \text{H.c.}\big) \tag{5.51}$$

The first term in the r.h.s. here can be interpreted as the voltage bias between the reservoirs of 1- and 2-particles, cf. Eq. (5.50), while the second term has an appearance of k-conserving tunneling with very small (proportional to $\theta_0 \ll 1$) tunneling amplitude.

Similar to Eq. (5.51), the current operator $\hat{I}$, see Eq. (5.18), splits naturally into two parts,

$$\begin{aligned}
&\hat{I} = \hat{I}_0 + \delta\hat{I},\\
&\hat{I}_0 = \frac{d}{dt}\frac{e}{2}\big(\hat{N}_1 - \hat{N}_2\big) = -ie^2V\theta_0 \sum_{ks}\psi^\dagger_{1ks}\psi_{2ks} + \text{H.c.},\\
&\delta\hat{I} = -e\,\theta_0\frac{d}{dt}\sum_{ks}\psi^\dagger_{1ks}\psi_{2ks} + \text{H.c.}
\end{aligned}$$

It turns out that $\delta\hat{I}$ does not contribute to the average current in the leading (second) order in θ_0 [47]. Indeed, in this order

$$\langle\delta\hat{I}\rangle = i\theta_0^2e^2V\frac{d}{dt}\int_{-\infty}^{t}dt'\left\langle[\hat{\mathcal{O}}(t),\hat{\mathcal{O}}(t')]\right\rangle_0, \quad \hat{\mathcal{O}} = \sum_{ks}\psi^\dagger_{1ks}\psi_{2ks},$$

where $\langle\ldots\rangle_0$ denotes thermodynamic averaging with the Hamiltonian $H_{\text{eff}} + H_V(0)$. The thermodynamic (equilibrium) averaging is well defined here, because for $\theta_0 = 0$ the Hamiltonian $H_{\text{eff}} + H_V$ conserves separately the numbers of 1- and 2-particles. Taking into account that $\langle[\hat{\mathcal{O}}(t),\hat{\mathcal{O}}(t')]\rangle_0$ depends only on the difference $\tau = t - t'$, we find

$$\langle\delta\hat{I}\rangle = i\theta_0^2e^2V\frac{d}{dt}\int_0^{\infty}d\tau\left\langle[\hat{\mathcal{O}}(\tau),\hat{\mathcal{O}}(0)]\right\rangle_0 = 0.$$

The remaining contribution $I = \langle\hat{I}_0\rangle$ corresponds to tunneling current between two bulk reservoirs containing 1- and 2-particles. Its evaluation follows the standard procedure [71] and yields [47]

$$\frac{dI}{dV} = G_0\frac{1}{2}\sum_s\left[-\pi\nu\,\text{Im}\,T_s(eV)\right] \tag{5.52}$$

for the differential conductance across the dot at zero temperature. Here G_0 coincides with the small θ_0-limit of Eq. (5.22). Using now Eqs. (5.26), (5.27), and (5.46), we obtain

$$\frac{1}{G_0}\frac{dI}{dV} = \begin{cases} 1 - \dfrac{3}{2}\left(\dfrac{eV}{T_K}\right)^2, & |eV| \ll T_K \\ \dfrac{3\pi^2/16}{\ln^2(|eV|/T_K)}, & |eV| \gg T_K \end{cases} \tag{5.53}$$

Thus, a large voltage bias has qualitatively the same destructive effect on the Kondo physics as the temperature does. The result Eq. (5.53) remains valid as long as $T \ll |eV| \ll \delta E$. If temperature exceeds the bias, $T \gg eV$, the differential conductance coincides with the linear conductance, see Eqs. (5.28) and (5.47) above.

5.6. Splitting of the Kondo peak in a magnetic field

According to Eq. (5.53), the differential conductance exhibits a peak at zero bias. The very appearance of such peak, however, does not indicate that we are dealing with the Kondo effect. Indeed, even in the absence of interactions, tunneling via a resonant level situated at the Fermi energy would also result in a zero-bias peak in dI/dV. These two situations can be distinguished by considering the evolution of the zero-bias peak with the magnetic field. In both cases, a sufficiently strong field (such that the corresponding Zeeman energy B appreciably exceeds the peaks width) splits the zero-bias peak in two smaller ones, located at $\pm V^*$. In the case of conventional resonant tunneling, $eV^* = B/2$. However, if the split peaks are of the Kondo origin, then $eV^* \approx B$. This doubling of the distance between the split peaks is viewed by many as a hallmark of the many-body physics associated with the Kondo effect [4].

In order to address the splitting of the zero-bias Kondo peak we add to the Hamiltonian (5.12) a term

$$H_B = BS_z + \sum_{ks} \frac{Bs}{2}\psi^\dagger_{1ks}\psi_{1ks} \tag{5.54}$$

describing the Zeeman effect of the magnetic field[7]. We concentrate on the most

[7] In general, magnetic field affects both the orbital and spin parts of the electronic wave function. However, as long as spin of the dot remains equal $1/2$ (the opposite case is considered in the next Section), the orbital effect of the field is unimportant. It modifies the exchange amplitude J and the bandwidth Δ in the Hamiltonian (5.12), which may eventually alter the values of G_0 and T_K in Eq. (5.53). However, the functional form of the dependence of dI/dV on V at a fixed B remains intact.

interesting case of

$$T_K \ll B \ll \Delta. \tag{5.55}$$

The first inequality here ensures that the zero-bias peak is split, while the second one allows the development of the Kondo correlations to a certain extend. For simplicity, we also consider here a strongly asymmetric setup, as in Section 5.5, which allows us to use Eq. (5.52) relating the differential conductance to the t-matrix. Note, however, that the results presented below remain qualitatively correct even when this assumption is lifted.

As long as the bias $|eV|$ is small compared to B, the differential conductance approximately coincides with the linear one, see Eq. (5.49). Similarly, at $|eV| \gg B$ the field has a negligible effect, and dI/dV is given by the second line in Eq. (5.53). The presence of the field, however, significantly affects the dependence of dI/dV on V at $|eV| \sim B \gg T$, and it is this regime that we address here.

Clearly, for $B \sim |eV| \gg T_K$ the system is in the weak coupling Kondo regime, so that the perturbative RG procedure described in Section 5.3 is an adequate tool to study it. Let us suppose, for simplicity, that in the absence of magnetic field electrons are filling the lower half of a band characterized by width 2Δ and constant density of states ν, see Fig. 4(a). In the presence of the field, the energy of an itinerant electron consists of the orbital part ξ_k and the Zeeman energy $Bs/2$, see the second term in Eq. (5.54). Condition $\xi_k + Bs/2 = \epsilon_F$ cuts out different strips of orbital energies for spin-up and spin-down electrons, see Fig. 4(b). To set the stage for the RG, it is convenient to cut the initial band asymmetrically for spin-up and spin-down electrons. The resulting band structure, shown in Fig. 4(c), is the same for both directions of spin. Further symmetric reductions of the band in the course of RG leave this band structure intact.

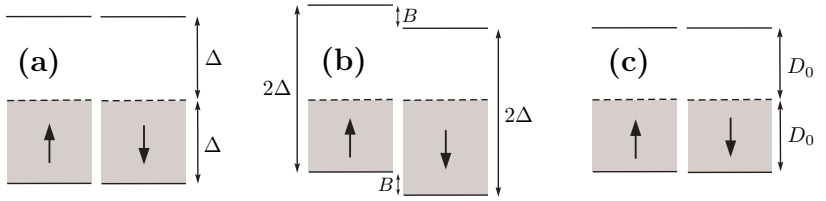

Fig. 4. The energy bands for spin-up and spin-down itinerant electrons. The solid lines denote the boundaries of the bands, the dashed lines correspond to the Fermi energy.
(a) Band structure without Zeeman splitting; (b) same with $B \neq 0$; (c) same after the initial asymmetric cutting of the bands ($D_0 = \Delta - B$).

After the initial cutting of the band, the effective Hamiltonian $H_{\rm eff} + H_B$

assumes the form

$$H = \sum_{ks} \xi_k \psi^\dagger_{ks} \psi_{ks} + J(\mathbf{s}_\psi \cdot \mathbf{S}) + \eta B S^z. \tag{5.56}$$

Here k is measured from the Fermi momentum of electrons with spin s, and we suppressed the subscript 1 in the operators ψ_{1ks} etc. The Hamiltonian (5.56) is defined within a symmetric band

$$|\xi_k| < D_0 = \Delta - B \approx \Delta,$$

see Fig. 4(c). The parameter η in (5.56) is given by

$$\eta = 1 - \nu J/2 \tag{5.57}$$

with J being the "bare" value of the exchange constant. The correction $-\nu J/2$ in Eq. (5.57) is nothing else but the Knight shift [72]. In a finite magnetic field, there are more spin-down electrons than spin-up ones, see Fig. 4(b). This mismatch results in a non-zero ground state expectation value $\langle s^z_1 \rangle = -\nu B/2$ of the operator s^z_1 in Eq. (5.12). Due to the exchange interaction, this induces an additional effective magnetic field $-\nu J B/2$ acting on the localized spin.

The form of the effective Hamiltonian (5.56) remains invariant under the RG transformation. The evolution of J and η with the reduction of the bandwidth D is governed by the equations

$$\frac{dJ_D}{d\zeta} = \nu J_D^2, \tag{5.58}$$

$$\frac{d \ln \eta_D}{d\zeta} = -\frac{1}{2}(\nu J_D)^2, \tag{5.59}$$

where $\zeta = \ln(\Delta/D)$. Equation (5.58) was derived in Section 5.3 above; the derivation of Eq. (5.59) proceeds in a similar way. It is clear from the solution of Eq. (5.58), see Eq. (5.32), that νJ_D remains small throughout the weak coupling regime $D \gg T_K$. It then follows from Eqs. (5.57) and (5.59) that η_D is of the order of 1 in this range of D. The renormalization described by Eqs. (5.58) and (5.59) must be terminated at $D \sim 2B \gg T_K$, so that $\eta_B B$ remains smaller than D. At this point

$$\nu J_B = \frac{1}{\ln(B/T_K)}\,, \tag{5.60}$$

see Eq. (5.32). Solution of Eq. (5.59) in the scaling limit[8], defined as

$$\frac{\ln(B/T_K)}{\ln(\Delta/T_K)} \ll 1,$$

[8] In this limit the Knight shift in Eq. (5.57) can be neglected.

takes the familiar form [57]

$$\eta_B = 1 - \frac{1}{2\ln(B/T_K)}\,. \tag{5.61}$$

Now we are ready to evaluate the differential conductance. The Hamiltonian Eq. (5.56) with J and η given by Eqs. (5.60) and (5.61) is defined in a sufficiently wide band $D \sim 2B$ to allow for excitations with energy of the order of Zeeman splitting. Since the current operator remains invariant in the course of renormalization, the differential conductance can still be calculated from Eq. (5.52). In the lowest order in νJ_B (Born approximation) we find

$$\frac{1}{G_0}\frac{dI}{dV} = \frac{\pi^2/16}{\ln^2(B/T_K)}\Big[1 + 2\theta(|eV| - \eta_B B)\Big]. \tag{5.62}$$

The main new feature of Eq. (5.62) compared to (5.53) is a threshold behavior at $|eV| = \eta_B B$. The origin of this behavior is apparent: for $|eV| > \eta_B B$ an inelastic (spin-flip) scattering channel opens up, causing a step in dI/dV.

In the absence of Zeeman splitting, going beyond the Born approximation in the renormalized exchange amplitude Eq. (5.32) would be meaningless, as this would exceed the accuracy of the logarithmic RG. This largely remains true here as well, except when the bias is very close to the inelastic scattering threshold,

$$\Big||eV| - \eta_B B\Big| \ll B.$$

The existence of the threshold makes the t-matrix singular at $\omega = \eta_B B$; such logarithmically divergent contribution appears in the third order in J_B [50]. Retaining of this contribution does not violate the accuracy of our approximations, and we find

$$\begin{aligned}\frac{1}{G_0}\frac{dI}{dV} &= \frac{\pi^2/16}{\ln^2(B/T_K)}\Big[1 + 2\theta(|eV| - \eta_B B)\Big] \\ &\quad\times\left(1 + \frac{1}{\ln(B/T_K)}\ln\frac{B}{\big||eV| - \eta_B B\big|}\right).\end{aligned} \tag{5.63}$$

We see now that the zero-bias peak in the differential conductance is indeed split in two by the applied magnetic field. The split peaks are located at $\pm V^*$ with

$$V^* = \eta_B B = \left[1 - \frac{1}{2\ln(B/T_K)}\right] B\,, \tag{5.64}$$

see Eq. (5.61).

Because of the logarithmic divergence in Eq. (5.63) this result needs a refinement. A finite temperature $T \gg T_K$ would of course cut the divergence [50]; this amounts to the replacement of $\big||eV| - \eta_B B\big|$ under the logarithm in Eq. (5.63) by $\max\Big\{\big||eV| - \eta_B B\big|, T\Big\}$. This is fully similar to the cut-off of the zero-bias Kondo singularity in the absence of the field.

The $T = 0$ case, however, is different, and turns out to be much simpler than the $B = 0$ Kondo anomaly at zero bias. The logarithmic singularity in Eq. (5.63) is brought about by the second-order in J_B contribution to the scattering amplitude. This contribution involves a transition to the excited $(S^z = +1/2)$ state of the localized spin. Unlike the $B = 0$ case, now such a state has a finite lifetime: the spin of the dot may flip, exciting (a triplet) electron-hole pair of energy $\eta_B B$ in the band. Such relaxation mechanism was first considered by Korringa [73]. In our case the corresponding relaxation rate is easily found with the help of the Fermi Golden Rule,

$$\gamma_K = \frac{\pi}{2} \frac{\eta_B B}{\ln^2(B/T_K)}. \tag{5.65}$$

Due to the finite Korringa relaxation rate the state responsible for the logarithmic singularity is broadened by γ_K, which cuts off the divergence [74] in Eq. (5.63). It also smears the step-like dependence on V, which we found in the Born approximation, see Eq. (5.62). As a result, the split peaks in the $V-$dependence of dI/dV are broad and low. The width of the peaks is

$$\delta V \sim \gamma_K \sim \frac{B}{\ln^2(B/T_K)}\,, \tag{5.66}$$

and their height is given by

$$\frac{G(V^*) - G(0)}{G(0)} \sim \frac{\ln\left[\ln(B/T_K)\right]}{\ln(B/T_K)} \ll 1. \tag{5.67}$$

Here we used the short-hand notation $dI/dV = G(V)$. When evaluating $G(V^*)$, we replaced $\big||eV| - \eta_B B\big|$ by γ_K in the argument of the logarithm in Eq. (5.63). The right-hand side of Eq. (5.67) is small, and the higher-order in νJ_B corrections to it are negligible.

The problem of the field-induced splitting of the Kondo peak was revisited many times since the works of Appelbaum [50], see e.g. [75, 76, 77].

5.7. Kondo effect in quantum dots with large spin

If the dot's spin exceeds $1/2$, see Refs. [78, 79, 80], then, as discussed in Section 5.1 above, both exchange constants J_γ in the effective Hamiltonian (5.2) are

finite and positive. This turns out to have a dramatic effect on the dependence of the conductance in the Kondo regime on temperature T and on Zeeman energy B. Unlike the case of $S = 1/2$ on the dot, see Fig. 3, now the dependences on T and B are *non-monotonic*: initial increase of G follows by a drop when the temperature is lowered [33, 81] at $B = 0$; the variation of G with B at $T = 0$ is similarly non-monotonic.

The origin of this peculiar behavior is easier to understand by considering the B-dependence of the zero-temperature conductance [33]. We assume that the magnetic field $H_\parallel$ is applied *in the plane* of the dot. Such field leads to the Zeeman splitting B of the spin states of the dot, see Eq. (5.37), but barely affects the orbital motion of electrons.

At any finite B the ground state of the system is not degenerate. Therefore, the linear conductance at $T = 0$ can be calculated from the Landauer formula

$$G = \frac{e^2}{h} \sum_s \left| \mathbb{S}^2_{s;RL} \right|, \tag{5.68}$$

which relates G to the amplitude of scattering $\mathbb{S}_{s;RL}$ of an electron with spin s from lead L to lead R. The amplitudes $\mathbb{S}_{s;\alpha\alpha'}$ form 2×2 scattering matrix $\hat{\mathbb{S}}_s$. In the basis of "channels", see Eq. (5.2), this matrix is obviously diagonal, and its eigenvalues $\exp(2i\delta_{\gamma s})$ are related to the scattering phase shifts $\delta_{\gamma s}$. The scattering matrix in the original $(R - L)$ basis is obtained from

$$\hat{\mathbb{S}}_s = \hat{U}^\dagger \mathrm{diag} \left\{ e^{2i\delta_{\gamma s}} \right\} \hat{U},$$

where $\hat{U}$ is a matrix of a rotation by an angle θ_0, see Eq. (5.19). The Landauer formula (5.68) then yields

$$G = G_0 \frac{1}{2} \sum_s \sin^2 \left(\delta_{1s} - \delta_{2s} \right), \quad G_0 = \frac{2e^2}{h} \sin^2(2\theta_0), \tag{5.69}$$

which generalizes the single-channel expression (5.34).

Equation (5.69) can be further simplified for a particle-hole symmetric model (5.2). Indeed, in this case the phase shifts satisfy $\delta_{\gamma\uparrow} + \delta_{\gamma\downarrow} = 0$, cf. Eq. (5.36), which suggests a representation

$$\delta_{\gamma s} = s\delta_\gamma. \tag{5.70}$$

Substitution into Eq. (5.69) then results in

$$G = G_0 \sin^2 \left(\delta_1 - \delta_2 \right). \tag{5.71}$$

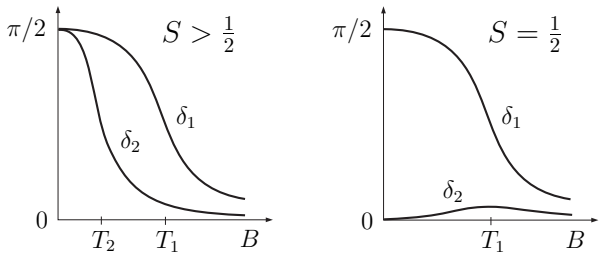

Fig. 5. Dependence of the scattering phase shifts at the Fermi level on the magnetic field for $S > 1/2$ (left panel) and $S = 1/2$ (right panel).

If spin on the dot S exceeds $1/2$, then both channels of itinerant electrons participate in the screening of the dot's spin [56]. Accordingly, in the limit $B \to 0$ both phase shifts δ_γ approach the unitary limit value $\pi/2$, see Fig. 5. However, the increase of the phase shifts with lowering the field is characterized by two different energy scales. These scales, the Kondo temperatures T_1 and T_2, are related to the corresponding exchange constants in the effective Hamiltonian (5.2),

$$\ln\left(\frac{\Delta}{T_\gamma}\right) \sim \frac{1}{\nu J_\gamma},$$

so that $T_1 > T_2$ for $J_1 > J_2$. It is then obvious from Eq. (5.71) that the conductance across the dot is small both at weak ($B \ll T_2$) and strong ($B \gg T_1$) fields, but may become large ($\sim G_0$) at intermediate fields $T_2 \ll B \ll T_1$, see Fig. 6. In other words, the dependence of zero-temperature conductance on the magnetic field is non-monotonic.

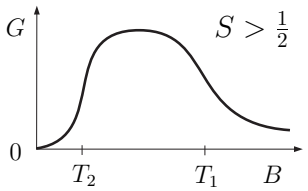

Fig. 6. Sketch of the magnetic field dependence of the Kondo contribution to the linear conductance at zero temperature. The conductance as function of temperature exhibits a similar non-monotonic dependence.

This non-monotonic dependence is in sharp contrast with the monotonic increase of the conductance with lowering the field when $S = 1/2$. Indeed, in the

latter case it is the channel whose coupling to the dot is the strongest that screens the dot's spin, while the remaining channel decouples at low energies [56], see Fig. 5.

The dependence of the conductance on temperature $G(T)$ is very similar[9] to $G(B)$. For example, for $S = 1$ one obtains [33]

$$G/G_0 = \begin{cases} (\pi T)^2 \left(\dfrac{1}{T_1} - \dfrac{1}{T_2}\right)^2, & T \ll T_2 \\ \dfrac{\pi^2}{2}\left[\dfrac{1}{\ln(T/T_1)} - \dfrac{1}{\ln(T/T_2)}\right]^2, & T \gg T_1 \end{cases} \tag{5.72}$$

The conductance reaches its maximun $G_{\max}$ at $T \sim \sqrt{T_1 T_2}$. The value of $G_{\max}$ can be found analytically for $T_1 \gg T_2$. For $S = 1$ the result reads [33]

$$G_{\max} = G_0 \left[1 - \frac{3\pi^2}{\ln^2(T_1/T_2)}\right]. \tag{5.73}$$

Consider now a Coulomb blockade valley with $N = \text{even}$ electrons and spin $S = 1$ on the dot. In a typical situation, the dot's spin in two neighboring valleys (with $N \pm 1$ electrons) is $1/2$. Under the conditions of applicability of the approximation Eq. (5.5), there is a single non-zero exchange constant $J_{N\pm1}$ for each of these valleys. If the Kondo temperatures T_K are the same for both valleys with $S = 1/2$, then $J_{N+1} = J_{N-1} = J_{\rm odd}$. Each of the two singly-occupied energy levels in the valley with $S = 1$ is also singly-occupied in one of the two neighboring valleys. It then follows from Eqs. (5.4)-(5.6) that the exchange constants $J_{1,2}$ for $S = 1$ satisfy

$$J_1 + J_2 = \frac{1}{2}\left(J_{N+1} + J_{N-1}\right) = J_{\rm odd}.$$

Since both J_1 and J_2 are positive, this immediately implies that $J_{1,2} < J_{\rm odd}$. Accordingly, both Kondo temperatures $T_{1,2}$ are expected to be smaller than T_K in the nearby valleys with $S = 1/2$.

This consideration, however, is not applicable when the dot is tuned to the vicinity of the singlet-triplet transition in its ground state [11, 12, 79, 80], i.e. when the energy gap Δ between the triplet ground state and the singlet excited state of an isolated dot is small compared to the mean level spacing δE. In this case the exchange constants in the effective Hamiltonian (5.2) should account for additional renormalization that the system's parameters undergo [82] when the high-energy cutoff (the bandwidth of the effective Hamiltonian) D is reduced

[9] Note, however, that $\langle \psi_1^\dagger(t)\psi_2(t)\psi_2^\dagger(0)\psi_1(0)\rangle \neq \langle \psi_1^\dagger(t)\psi_1(0)\rangle\langle \psi_2(t)\psi_2^\dagger(0)\rangle$ at finite T. Therefore, unlike Eq. (5.34), there is no simple generalization of Eq. (5.21) to the two-channel case.

from $D \sim \delta E$ down to $D \sim \Delta \ll \delta E$, see also [63]. The renormalization enhances the exchange constants $J_{1,2}$. If the ratio $\Delta/\delta E$ is sufficiently small, then the Kondo temperatures $T_{1,2}$ for $S = 1$ may become of the same order [78, 80], or even significantly exceed [11, 12, 79] the corresponding scale T_K for $S = 1/2$.

In GaAs-based lateral quantum dot systems the value of Δ can be controlled by a magnetic field $H_\perp$ applied *perpendicular to the plane* of the dot [79]. Because of the smallness of the effective mass m^*, even a weak field $H_\perp$ has a strong orbital effect. At the same time, smallness of the quasiparticle g-factor in GaAs ensures that the corresponding Zeeman splitting remains small [12]. Theory of the Kondo effect in lateral quantum dots in the vicinity of the singlet-triplet transition was developed in [83], see also [84].

6. Concluding remarks

In the simplest form of the Kondo effect considered in these notes, a quantum dot behaves essentially as an artificial "magnetic impurity" with spin S, coupled via exchange interaction to two conducting leads. The details of the temperature dependence $G(T)$ of the linear conductance across the dot depend on the dot's spin S. In the most common case of $S = 1/2$ the conductance in the Kondo regime monotonically increases with the decrease of temperature, potentially up to the quantum limit $2e^2/h$. Qualitatively (although not quantitatively), this increase can be understood from the Anderson impurity model in which the dot is described by a single energy level. On the contrary, when spin on the dot exceeds $1/2$, the evolution of the conductance proceeds in two stages: the conductance first raises, and then drops again when the temperature is lowered.

In a typical experiment [4], one measures the dependence of the differential conductance on temperature T, Zeeman energy B, and dc voltage bias V. When one of these parameters is much larger than the other two, and is also large compared to the Kondo temperature T_K, the differential conductance exhibits a logarithmic dependence

$$\frac{1}{G_0}\frac{dI}{dV} \propto \left[\ln \frac{\max\{T, B, eV\}}{T_K}\right]^{-2}, \tag{6.1}$$

characteristic for the weak coupling regime of the Kondo system, see Section 5.3. Consider now a zero-temperature transport through a quantum dot with $S = 1/2$ in the presence of a strong field $B \gg T_K$. In accordance with Eq. (6.1), the differential conductance is small compared to G_0 both for $eV \ll B$ and for $eV \gg B$. However, the calculation in the third order of perturbation theory

in the exchange constant yields a contribution that diverges logarithmically at $eV \approx \pm B$ [50]. The divergence is reminiscent of the Kondo zero-bias anomaly. However, the full development of resonance is inhibited by a finite lifetime of the excited spin state of the dot [74]. As a result, the peak in the differential conductance at $eV = \pm\mu B$ is broader and lower then the corresponding peak at zero bias in the absence of the field, see Section 5.6.

One encounters similar effects in studies of the influence of a weak ac signal of frequency $\Omega \gtrsim T_K$ applied to the gate electrode [85] on transport across the dot. In close analogy with the usual photon-assisted tunneling [86], such perturbation is expected to result in the formation of satellites [87] at $eV = n\hbar\Omega$ (here n is an integer) to the zero-bias peak in the differential conductance. Again, the resonances responsible for the formation of the satellite peaks are limited by the finite lifetime effects [88].

The spin degeneracy is not the only possible source of the Kondo effect in quantum dots. Consider, for example, a large dot connected by a single-mode junction to a conducting lead and tuned to the vicinity of the Coulomb blockade peak [31]. If one neglects the finite level spacing in the dot, then the two almost degenerate charge state of the dot can be labeled by a pseudospin, while real spin plays the part of the channel index [31, 89]. This setup turns out to be a robust realization [31, 89] of the symmetric (i.e. having equal exchange constants) two-channel $S = 1/2$ Kondo model [56]. The model results in a peculiar temperature dependence of the observable quantities, which at low temperatures follow power laws with manifestly non-Fermi-liquid fractional values of the exponents [90].

It should be emphasized that in the usual geometry consisting of two leads attached to a Coulomb-blockaded quantum dot with $S = 1/2$, only the conventional Fermi-liquid behavior can be observed at low temperatures. Indeed, in this case the two exchange constants in the effective exchange Hamiltonian (5.2) are vastly different, and their ratio is not tunable by conventional means, see the discussion in Section 5.1 above. A way around this difficulty was proposed in [91]. The key idea is to replace one of the leads in the standard configuration by a very large quantum dot, characterized by a level spacing $\delta E'$ and a charging energy E'_C. At $T \gg \delta E'$, particle-hole excitations within this dot are allowed, and electrons in it participate in the screening of the smaller dot's spin. At the same time, as long as $T \ll E'_C$, the number of electrons in the large dot is fixed. Therefore, the large dot provides for a separate screening channel which does not mix with that supplied by the remaining lead. In this system, the two exchange constants are controlled by the conductances of the dot-lead and dot-dot junctions. A strategy for tuning the device parameters to the critical point characterized by the two-channel Kondo physics is discussed in [92].

Finally, we should mention that the description based on the universal Hamiltonian (2.15) is not applicable to large quantum dots subjected to a *quantizing*

magnetic field $H_\perp$ [93, 94]. Such field changes drastically the way the screening occurs in a confined droplet of a two-dimensional electron gas [95]. The droplet is divided into alternating domains containing compressible and incompressible electron liquids. In the metal-like compressible regions, the screening is almost perfect. On the contrary, the incompressible regions behave very much like insulators. In the case of lateral quantum dots, a large compressible domain is formed near the center of the dot. The domain is surrounded by a narrow incompressible region separating it from another compressible ring-shaped domain formed along the edges of the dot [96]. This system can be viewed as two concentric capacitively coupled quantum "dots" - the core dot and the edge dot [93, 96]. When the leads are attached to the edge dot, the measured conductance is sensitive to its spin state: when the number of electrons in the edge dot is odd, the conductance becomes large due to the Kondo effect [93]. Changing the field causes redistribution of electrons between the core and the edge, resulting in a striking checkerboard-like pattern of high- and low-conductance regions [93, 94]. This behavior persists as long as the Zeeman energy remains small compared to the Kondo temperature. Note that compressible regions are also formed around an *antidot* – a potential hill in a two-dimensional electron gas in the quantum Hall regime [97]. Both Coulomb blockade oscillations and Kondo-like behavior were observed in these systems [98].

Kondo effect arises whenever a coupling to a Fermi gas induces transitions within otherwise degenerate ground state multiplet of an interacting system. Both coupling to a Fermi gas and interactions are naturally present in a nanoscale transport experiment. At the same time, many nanostructures can be easily tuned to the vicinity of a degeneracy point. This is why the Kondo effect in its various forms often influences the low temperature transport in meso- and nanoscale systems.

In these notes we reviewed the theory of the Kondo effect in transport through quantum dots. A Coulomb-blockaded quantum dot behaves in many aspects as an artificial "magnetic impurity" coupled via exchange interaction to two conducting leads. Kondo effect in transport through such "impurity" manifests itself in the lifting of the Coulomb blockade at low temperatures, and, therefore, can be unambiguously identified. Quantum dot systems not only offer a direct access to transport properties of an artificial impurity, but also provide one with a broad arsenal of tools to tweak the impurity properties, unmatched in conventional systems. The characteristic energy scale for the intra-dot excitations is much smaller than the corresponding scale for natural magnetic impurities. This allows one to induce degeneracies in the ground state of a dot which are more exotic than just the spin degeneracy. This is only one out of many possible extensions of the simple model discussed in these notes.

7. Acknowledgements

This project was supported by NSF grants DMR02-37296 and EIA02-10736, and by the Nanoscience/Nanoengineering Research Program of Georgia Tech.

References

[1] L.P. Kouwenhoven et al., in: *Mesoscopic Electron Transport*, eds. L.L. Sohn et al., (Kluwer, Dordrecht, 1997), p. 105; M.A. Kastner, Rev. Mod. Phys. **64** (1992) 849; U. Meirav and E.B. Foxman, Semicond. Sci. Technol. **11** (1996) 255; L.P. Kouwenhoven and C.M. Marcus, Phys. World **11** (1998) 35.

[2] P. Joyez et al., Phys. Rev. Lett. **79** (1997) 1349; M. Devoret and C. Glattli, Phys. World **11** (1998) 29.

[3] B.L. Altshuler and A.G. Aronov, in: *Electron-Electron Interactions in Disordered Systems*, eds. A.L. Efros and M. Pollak (North-Holland, Amsterdam, 1985), p. 1.

[4] D. Goldhaber-Gordon et al., Nature **391** (1998) 156; S.M. Cronenwett, T.H. Oosterkamp and L.P. Kouwenhoven, Science **281** (1998) 540; J. Schmid et al., Physica B **256-258** (1998) 182.

[5] L. Kouwenhoven and L. Glazman, Physics World **14** (2001) 33.

[6] J. Kondo, Prog. Theor. Phys. **32** (1964) 37.

[7] Furusaki A and K.A. Matveev Phys. Rev. B **52** (1995) 16676.

[8] I.L. Aleiner and L.I. Glazman, Phys. Rev. B **57** (1998) 9608.

[9] S.M. Cronenwett et al., Phys. Rev. Lett. **81** (1998) 5904.

[10] S. Tarucha et al., Phys. Rev. Lett. **84** (2000) 2485; L.P. Kouwenhoven, D.G. Austing and S. Tarucha, Rep. Prog. Phys. **64** (2001) 701.

[11] S. Sasaki et al., Nature **405** (2000) 764; S. Sasaki et al., Phys. Rev. Lett. **93** (2004) 017205.

[12] M. Pustilnik et al., Lecture Notes in Physics **579** (2001) 3 (cond-mat/0010336).

[13] J. Nygård, D.H. Cobden and P.E. Lindelof, Nature **408** (2000) 342; W. Liang, M. Bockrath and H. Park, Phys. Rev. Lett. **88** (2002) 126801; B. Babić, T. Kontos and C. Schönenberger, cond-mat/0407193.

[14] J. Park et al., Nature **417** (2002) 722; W. Liang et al., Nature **417** (2002) 725; L.H. Yu and D. Natelson, Nano Lett. **4** (2004) 79.

[15] L.T. Li et al., Phys. Rev. Lett. **80** (1998) 2893; V. Madhavan et al., Science **280** (1998) 567; H.C. Manoharan et al., Nature **403** (2000) 512.

[16] M.V. Berry, Proc. R. Soc. A **400** (1985) 229; B.L. Altshuler and B.I. Shklovskii, Zh. Eksp. Teor. Fiz. **91** (1986) 220 [Sov. Phys.–JETP **64** (1986) 127].

[17] C.W.J. Beenakker, Rev. Mod. Phys. **69** (1997) 731.

[18] Y. Alhassid, Rev. Mod. Phys. **72** (2000) 895.

[19] F. Haake, *Quantum Signatures of Chaos* (Springer-Verlag, New York, 2001).

[20] K. Efetov, *Supersymmetry in Disorder and Chaos* (Cambridge University Press, Cambridge, 1997).

[21] B.L. Altshuler et al.,Phys. Rev. Lett. **78** (1997) 2803; O. Agam et al., Phys. Rev. Lett. **78** (1997) 1956; Ya.M. Blanter, Phys. Rev. B **54** (1996) 12807; Ya.M. Blanter and A.D. Mirlin, Phys. Rev. B **57** (1998) 4566; Ya.M. Blanter, A.D. Mirlin and B.A. Muzykantskii, Phys. Rev. Lett. **78** (1997) 2449; I.L. Aleiner and L.I. Glazman, Phys. Rev. B **57** (1998) 9608.

[22] I.L. Kurland, I.L. Aleiner and B.L. Altshuler, Phys. Rev. B **62** (2000) 14886.

[23] I.L. Aleiner, P.W. Brouwer and L.I. Glazman, Phys. Rep. **358** (2002) 309.

[24] M.V. Berry, Journ. of Phys. A **10** (1977) 2083; Ya.M. Blanter and A.D. Mirlin, Phys. Rev. E **55** (1997) 6514 Ya.M. Blanter, A.D. Mirlin and and B.A. Muzykantskii, Phys. Rev. B **63** (2001) 235315; A.D. Mirlin, Phys. Rep. **326** (2000) 259.

[25] J.A. Folk et al., Phys. Rev. Lett. **76** (1996) 1699.

[26] J.M. Ziman, *Principles of the Theory of Solids* (Cambridge University Press, Cambridge, 1972), p. 339.

[27] J. von Delft and D.C. Ralph, Phys. Rep. **345** (2001) 61.

[28] K.A. Matveev, L.I. Glazman and R.I. Shekhter, Mod. Phys. Lett. B **8** (1994) 1007.

[29] P.W. Brouwer, Y. Oreg and B.I. Halperin, Phys. Rev. B **60** (1999) R13977; H.U. Baranger, D. Ullmo and L.I. Glazman, Phys. Rev. B **61** (2000) R2425.

[30] R.M. Potok et al., Phys. Rev. Lett. **91** (2003) 016802; J.A. Folk et al., Phys. Scripta **T90** (2001) 26; S. Lindemann et al., Phys. Rev. B **66** (2002) 195314.

[31] K.A. Matveev, Phys. Rev. B **51** (1995) 1743.

[32] K. Flensberg, Phys. Rev. B **48** (1993) 11156.

[33] M. Pustilnik and L.I. Glazman, Phys. Rev. Lett. **87** (2001) 216601.

[34] C.E. Porter and R.G. Thomas, Phys. Rev. **104** (1956) 483.

[35] I.O. Kulik and R.I. Shekhter, Zh. Eksp. Teor. Fiz. **62** (1975) 623 [Sov. Phys.–JETP **41** (1975) 308]; L.I. Glazman and R.I. Shekhter, Journ. of Phys.: Condens. Matter **1** (1989) 5811.

[36] L.I. Glazman and K.A. Matveev, Pis'ma Zh. Exp. Teor. Fiz. **48**, 403 (1988) [JETP Lett. **48**, 445 (1988)]; C.W.J. Beenakker, Phys. Rev. B **44** (1991) 1646; D.V. Averin, A.N. Korotkov and K.K. Likharev, Phys. Rev. B **44**, (1991) 6199.

[37] R.A. Jalabert, A.D. Stone and Y. Alhassid, Phys. Rev. Lett. **68** (1992) 3468.

[38] V.N. Prigodin, K.B. Efetov and S. Iida, Phys. Rev. Lett. **71** (1993) 1230.

[39] A.M. Chang et al., Phys. Rev. Lett. **76** (1996) 1695.

[40] B.L. Altshuler et al., Phys. Rev. B **22** (1980) 5142; S. Hikami, A.I. Larkin and Y. Nagaoka, Progr. Theor. Phys. **63** (1980) 707.

[41] I. Giaever and H.R. Zeller, Phys. Rev. Lett. **20** (1968) 1504; H.R. Zeller and I. Giaever, Phys. Rev. **181** (1969) 789.

[42] D.V. Averin and Yu.V. Nazarov, Phys. Rev. Lett. **65** (1990) 2446.

[43] A.A. Abrikosov, *Fundamentals of the Theory of Metals* (North-Holland, Amsterdam, 1988), p. 620.

[44] I.L. Aleiner and L.I. Glazman, Phys. Rev. Lett. **77** (1996) 2057.

[45] L.I. Glazman and M.E. Raikh, Pis'ma Zh. Eksp. Teor. Fiz. **47** (1988) 378 [JETP Lett. **47** (1988) 452]; T.K. Ng and P.A. Lee, Phys. Rev. Lett. **61** (1988) 1768.

[46] W.G. van der Wiel et al., Science **289** (2000) 2105; Y. Ji, M. Heiblum and H. Shtrikman, Phys. Rev. Lett. **88** (2002) 076601.

[47] L.I. Glazman and M. Pustilnik, in: *New Directions in Mesoscopic Physics (Towards Nanoscience)* eds. R. Fazio et al., (Kluwer, Dordrecht, 2003), p. 93 (cond-mat/0302159).

[48] C.B. Duke, *Tunneling in Solids* (Academic Press, New York, 1969); J.M. Rowell, in: *Tunneling Phenomena in Solids*, eds. E. Burstein and S. Lundqvist (Plenum Press, New York, 1969), p. 385.

[49] A.F.G. Wyatt, Phys. Rev. Lett. **13** (1964) 401; R.A. Logan and J.M. Rowell, Phys. Rev. Lett. **13** (1964) 404.

[50] J. Appelbaum, Phys. Rev. Lett. **17** (1966) 91; J.A. Appelbaum, Phys. Rev. **154** (1967) 633.

[51] P.W. Anderson, Phys. Rev. Lett. **17** (1966) 95.

[52] G.A. Fiete et al., Phys. Rev. B **66** (2002) 024431.

[53] M. Pustilnik and L.I. Glazman, Journ. of Physics: Condens. Matter **16** (2004) R513.

[54] J.R. Schrieffer and P.A. Wolff, Phys. Rev. **149** (1966) 491.

[55] P.G. Silvestrov and Y. Imry, Phys. Rev. Lett. **85** (2000) 2565.

[56] P. Nozières and A. Blandin, J. Physique **41** (1980) 193.

[57] P. Coleman, in: *Lectures on the Physics of Highly Correlated Electron Systems VI*, ed. F. Mancini (American Institute of Physics, New York, 2002), p. 79 (cond-mat/0206003); A.S. Hewson, *The Kondo Problem to Heavy Fermions* (Cambridge University Press, Cambridge, 1997).

[58] P.W. Anderson, *Basic Notions of Condensed Matter Physics* (Addison-Wesley, Reading, 1997).

[59] K.G. Wilson, Rev. Mod. Phys. **47** (1975) 773.

[60] L.I. Glazman, F.W.J. Hekking and A.I. Larkin, Phys. Rev. Lett. **83** (1999) 1830.

[61] A.M. Tsvelick and P.B. Wiegmann, Adv. Phys. **32** (1983) 453; N. Andrei, K. Furuya and J.H. Lowenstein, Rev. Mod. Phys. **55** (1983) 331.

[62] I. Affleck and A.W.W. Ludwig, Phys. Rev. B **48** (1993) 7297.

[63] M. Pustilnik and L.I. Glazman, Phys. Rev. B **64** (2001) 045328.

[64] A.A. Abrikosov, Physics **2** (1965) 5; A.A. Abrikosov, Usp. Fiz. Nauk **97** (1969) 403 [Sov. Phys.–Uspekhi **12** (1969) 168]; H. Suhl, Phys. Rev. **138** (1965) A515.

[65] R.G. Newton, *Scattering Theory of Waves and Particles* (Dover, Mineola, 2002).

[66] P.W. Anderson, Journ. of Physics C **3** (1970) 2436.

[67] P.W. Anderson, G. Yuval and D.R. Hamann, Phys. Rev. B **1** (1970) 4464.

[68] F. Wegner, Ann. Phys. **3** (1994) 77; Nucl. Phys. B **90** (2000) 141; S.D. Glazek and K.G. Wilson, Phys. Rev. D **49** (1994) 4214; Phys. Rev. D **57** (1998) 3558.

[69] P. Nozières, J. Low Temp. Phys. **17** (1974) 31; P. Nozières, in *Proceedings of the 14th International Conference on Low Temperature Physics*, eds. M. Krusius and M. Vuorio (North Holland, Amsterdam, 1974), Vol. 5, pp. 339-374; P. Nozières, J. Physique **39** (1978) 1117.

[70] T.A. Costi, A.C. Hewson and V. Zlatić, Journ. of Physics: Condens. Matter **6** (1994) 2519.

[71] G.D. Mahan, *Many-Particle Physics* (Plenum, New York, 1990).

[72] W.D. Knight, Phys. Rev. **76** (1949) 1259; C. H. Townes, C. Herring, and W. D. Knight, Phys. Rev. **77** (1950) 736.

[73] J. Korringa, Physica (Amsterdam) **16** (1950) 601.

[74] D.L. Losee and E.L. Wolf, Phys. Rev. Lett. **23** (1969) 1457.

[75] Y. Meir, N.S. Wingreen and P.A. Lee, Phys. Rev. Lett. **70** (1993) 2601.

[76] J.E. Moore and X.-G. Wen, Phys. Rev. Lett. **85** (2000) 1722.

[77] J. Paaske, A. Rosch, and P. Wölfle, Phys. Rev. B **69** (2004) 155330.

[78] J. Schmid et al., Phys. Rev. Lett. **84** (2000) 5824.

[79] W.G. van der Wiel et al., Phys. Rev. Lett. **88** (2002) 126803.

[80] A. Kogan et al., Phys. Rev. B **67** (2003) 113309.

[81] W. Izumida, O. Sakai and Y. Shimizu, J. Phys. Soc. Jpn. **67** (1998) 2444.

[82] M. Eto and Yu.V. Nazarov, Phys. Rev. Lett. **85** (2000) 1306; M. Pustilnik and L.I. Glazman, Phys. Rev. Lett. **85** (2000) 2993.

[83] V.N. Golovach and D. Loss, Europhys. Lett. **62** (2003) 83; M. Pustilnik, L.I. Glazman and W. Hofstetter, Phys. Rev. B **68** (2003) 161303(R).

[84] M. Pustilnik, Y. Avishai and K. Kikoin, Phys. Rev. Lett. **84** (2000) 1756.

[85] J.M. Elzerman et al., J. Low Temp. Phys. **118** (2000) 375.

[86] P.K. Tien and J.P. Gordon, Phys. Rev. **129** (1963) 647.

[87] M.H. Hettler and H. Schoeller, Phys. Rev. Lett. **74** (1995) 4907.

[88] A. Kaminski, Yu.V. Nazarov and L.I. Glazman, Phys. Rev. Lett. **83** (1999) 384; A. Kaminski, Yu.V. Nazarov and L.I. Glazman, Phys. Rev. B **62** (2000) 8154.

[89] K.A. Matveev, Zh. Eksp. Teor. Fiz. **99** (1991) 1598 [Sov. Phys.–JETP **72** (1991) 892].

[90] D.L. Cox and A. Zawadowski, Adv. Phys. **47** (1998) 599.

[91] Y. Oreg and D. Goldhaber-Gordon, Phys. Rev. Lett. **90** (2003) 136602.

[92] M. Pustilnik et al., Phys. Rev. B **69** (2004) 115316.

[93] M. Keller et al., Phys. Rev. B **64** (2001) 033302; M. Stopa et al., Phys. Rev. Lett. **91** (2003) 046601.

[94] S.M. Maurer et al., Phys. Rev. Lett. **83** (1999) 1403; D. Sprinzak et al., Phys. Rev. Lett. **88** (2002) 176805; C. Fühner et al., Phys. Rev. B **66** (2002) 161305(R).

[95] C.W.J. Beenakker, Phys. Rev. Lett. **64** (1990) 216; A.M. Chang, Solid State Commun. **74** (1990) 871; D.B. Chklovskii, B.I. Shklovskii and L.I. Glazman, Phys. Rev. B **46** (1992) 4026.

[96] P.L. McEuen et al., Phys. Rev. B **45** (1992) 11419; A.K. Evans, L.I. Glazman and B.I. Shklovskii, Phys. Rev. B **48** (1993) 11120.

[97] V.J. Goldman and B. Su, *Science* **267** (1995) 1010.

[98] M. Kataoka et al., Phys. Rev. Lett. **83** (1999) 160; M. Kataoka et al., Phys. Rev. Lett. **89** (2002) 226803.